Selection originating from protein foldability: II. Folding free energy, sequence ensemble, and fitness

Sanzo Miyazawa

arXiv:1612.09379v1 [q-bio.PE] 30 Dec 2016

Abstract

Assuming that mutation and fixation processes are reversible Markov processes, we prove that the equilibrium ensemble of sequences obeys a Boltzmann distribution with $\exp(4N_e m(1-1/(2N)))$, where m is a Malthusian fitness and N_e and N are the effective and actual population sizes. Combining this finding with the knowledge of protein folding, we derive a correspondence between protein fitness and folding free energy, i.e., $4N_e m(1-1/(2N))$ and $-\Delta G_{ND}/k_B T_s$, where $\Delta G_{ND} \equiv G_N - G_D$, G_N and G_D are the native and denatured free energies, and T_s is the effective temperature of natural selection. In the preceding manuscript, we analyzed dimensionless free energy changes, $\Delta\psi_N (= \Delta G_N/k_B T_s)$, due to single nucleotide nonsynonymous substitutions, for which the total interaction ψ_N of a sequence was estimated as the sum of one-body and pairwise interactions from a multiple sequence alignment. T_s for various protein families were estimated on the basis that the mean of $\Delta\psi_N$ over all sites is negatively proportional to ψ_N but their variance is nearly constant across homologous sequences. Based on these findings, we study the equilibrium state of protein foldability/stability in a monoclonal approximation, in which protein evolution proceeds with single amino acid substitutions fixed at a time in a population. The ensemble of proteins attains the equilibrium, $\psi_N = \psi_N^{\rm eq}$, where the average of $\Delta\psi_N$ over fixed mutants is equal to zero. Approximating the probability density function (PDF) of $\Delta\psi_N$ by a log-normal distribution, the PDF of $\Delta\psi_N (\simeq \Delta\Delta\psi_{ND})$ in fixed mutants is estimated. $\psi_N^{\rm eq}$ for 14 protein domains agree well with ψ_N averaged over homologous sequences. The PDFs of K_a/K_s, which is the ratio of nonsynonymous to synonymous substitution rate per site, at equilibrium confirm that T_s negatively correlates with the amino acid substitution rate. Contrary to the neutral theory, neutral selection is not significant even in fixed mutants.

Insert Received for publication Date and in final form Date.

sanzo.miyazawa@gmail.com

© 2013 The Authors
0006-3495/08/09/2624/12 $2.00 doi: 10.1529/biophysj.106.090944

Natural proteins can fold their sequences into unique structures. Protein's stability and foldability result from natural selection and are not typical characteristics of random polymers (1–3). Natural selection maintains protein's stability and foldability over evolutionary timescales. On the basis of the random energy model (REM) for protein folding, Pande et al. (3) discussed that the equilibrium ensemble of natural protein sequences is a canonical ensemble characterized by a Boltzmann factor $\exp(-\Delta G_{ND}(\boldsymbol{\sigma})/k_BT_s)$, where $\Delta G_{ND}(\boldsymbol{\sigma})(\equiv G_N(\boldsymbol{\sigma}) - G_D(\boldsymbol{\sigma}))$ is the folding free energy of sequence $\boldsymbol{\sigma}$, G_N and G_D are the free energies of native and denatured states, k_B is the Boltzmann constant, and T_s is the effective temperature of selection and must satisfy $T_s < T_g < T_m$ for natural proteins to fold into unique native structures; T_g is glass transition temperature and T_m is melting temperature; see the Methods section in the Supporting Material for details. The REM also indicates that the free energy of denatured conformations (G_D) is a function of amino acid frequencies only and does not depend on amino acid order, and therefore the Boltzmann factor will be taken as $\exp(-G_N(\boldsymbol{\sigma})/k_BT_s)$, if amino acid frequencies are kept constant.

On the other hand, the maximum entropy principle insists that the probability distribution of sequences in sequence space, which is characterized by the constraints on amino acid compositions at all sites and on amino acid pairwise frequencies for all site pairs, is a Boltzmann distribution with the Boltzmann factor $\exp(-\psi_N(\boldsymbol{\sigma}))$, where $\psi_N(\boldsymbol{\sigma})$ is the total interaction of a native sequence $\boldsymbol{\sigma}$ and represented as the sum of one-body (h) and pairwise (J) interactions between residues in the sequence; see the Methods section in the Supporting Material for details. The one-body (h) and pairwise (J) residue-residue interactions that satisfy those constraints for homologous sequences have been estimated (4–7) as one of Potts problems and successfully used to predict contacting residue pairs in protein structures (4–10).

We establish relationships between protein foldability/stability, sequence distribution, and protein fitness. First, we prove that if mutation and fixation processes in protein evolution are reversible Markov processes, the equilibrium ensemble of genes will obey a Boltzmann distribution with the Boltzmann factor $\exp(4N_em(1-1/(2N)))$, where N_e and N are effective and actual population sizes, and m is the Malthusian fitness of a gene. In other words, correspondences between $-\Delta G_{ND}/k_BT_s$, $-\Delta\psi_{ND}(\equiv \psi_N - \psi_D)$ and $4N_em(1-1/(2N))$ are obtained by equating these three Boltzmann distributions with each other; $\psi_D = G_D/k_BT_s +$ constant.

In the preceding manuscript (11), We examined the changes of ψ_N due to single nucleotide nonsynonymous substitutions over all sites in the homologous sequences of 14 protein families, and found the following regression equation.

$$\overline{\Delta\psi_N} \approx \alpha_{\psi_N}\frac{\psi_N - \overline{\psi_N}}{L} + \overline{\overline{\Delta\psi_N}} \qquad \text{with } \alpha_{\psi_N} < 0 \tag{1}$$

with correlation coefficients, $r_{\psi_N} > 0.9$, where L is sequence length, $\overline{\psi_N}$ denotes the average of ψ_N over all homologous sequences, and $\overline{\Delta\psi_N}$ and $\overline{\overline{\Delta\psi_N}}$ denote the average of $\Delta\psi_N$ over all single nucleotide synonymous substitutions at all sites in a protein sequence and its total average over all homologous sequences in a protein family, respectively. In addition, the following relationship for the variance of $\Delta\psi_N$ was found.

$$\begin{aligned} \mathrm{Var}(\Delta\psi_N) &\approx \text{independent of } \psi_N \text{ and} \\ &\quad \text{constant across homologous sequences in every protein family} \qquad (2) \\ &= \text{function of } k_BT_s \qquad (3) \end{aligned}$$

Because

$$\mathrm{Var}(\Delta G_N) = \text{function that must not explicitly depend on } k_BT_s \text{ but } G_N \tag{4}$$

the following important relationship was derived and used to estimate the relative value of T_s against $T_{s,\mathrm{PDZ}}$ of the PDZ family.

$$\begin{aligned} \mathrm{Var}(\Delta G_N) &= (k_BT_s)^2\mathrm{Var}(\Delta\psi_N) \\ &\approx \text{constant} \qquad (5) \end{aligned}$$

where $\mathrm{Var}(\Delta G_N)$ and $\mathrm{Var}(\Delta\psi_N)$ are the variances of ΔG_N and $\Delta\psi_N$ over all single nucleotide nonsynonymous substitutions at all sites, respectively. These relationships, Eqs. 1 and 5, are also shown in Figs. S3 and S4 , and the regression coefficients (α_{ψ_N}) and correlation coefficients (r_{ψ_N}) are listed in Tables S2 and S5. With estimated T_s and experimental melting temperature T_m, glass transition temperature T_g and folding free energy ΔG_N were estimated for each protein family on the basis of the REM. The estimates of T_s and T_g are all within a reasonable range, and the estimated values of ΔG_N agree well with their experimental values for 5 protein families, justifying the estimates of T_s.

Here, we study an amino acid substitution process in protein evolution, which is characterized by the fitness, $m = -\Delta\psi_{ND}/(4N_e(1-1/(2N)))$. We employ a monoclonal approximation for mutation and fixation processes of genes, in which

protein evolution proceeds with single amino acid substitutions fixed at a time in a population. In this approximation, ψ_N of a protein gene attains the equilibrium, $\psi_N = \psi_N^{\rm eq}$, when the average of $\Delta\psi_N (\simeq \Delta\Delta\psi_{ND})$ over singe nucleotide nonsynonymous mutations fixed in a population is equal to zero. Approximating the distribution of $\Delta\psi_N$ due to singe nucleotide nonsynonymous mutations by a log-normal distribution, their distribution for fixed mutants is numerically calculated and used to calculate the averages of various quantities and also the probability density functions (PDF) of K_a/K_s in all mutants and in fixed mutants; K_a/K_s is defined as the ratio of nonsynonymous to synonymous substitution rate per site. The Boltzmann distribution for the equilibrium ensemble of homologous sequences and the monoclonal approximation for mutation and fixation processes are both supported by a good agreement between the time average ($\psi_N^{\rm eq}$) and ensemble average ($\langle\psi_N\rangle_\sigma$), which is equal to the sample average, $\overline{\psi_N}$, of ψ_N over homologous sequences.

We also study protein evolution at equilibrium, $\psi_N = \psi_N^{\rm eq}$. The common understanding of protein evolution has been that amino acid substitutions observed in homologous proteins are neutral (12–15) or slightly deleterious (16, 17), and random drift is a primary force to fix amino acid substitutions in population. The PDFs of K_a/K_s in all arising mutations and in their fixed mutations are examined to see how significant each of positive, neutral, slightly negative,and negative selections is. Interestingly, stabilizing mutations are significantly fixed in population by positive selection, and balance with destabilizing mutations that are also significantly fixed by random drift, although most negative mutations are removed from population. Contrary to the neutral theory (12–15), the proportion of neutral selection is not large even in fixed mutants. It is also confirmed that the effective temperature (T_s) of selection negatively correlates with the amino acid substitution rate (K_a/K_s) of protein at equilibrium.

1 Methods

1.1 The equilibrium distribution of sequences in a mutation-fixation process

Here we assume that the mutational process is a reversible Markov process. That is, the mutation rate per gene, $M_{\boldsymbol{\mu\nu}}$, from sequence $\boldsymbol{\mu} \equiv (\mu_1, \cdots, \mu_L)$ to $\boldsymbol{\nu}$ satisfies the detailed balance condition

$$P^{\rm mut}(\boldsymbol{\mu}) M_{\mu\nu} \quad = \quad P^{\rm mut}(\boldsymbol{\nu}) M_{\nu\mu} \tag{6}$$

where $P^{\rm mut}(\boldsymbol{\nu})$ is the equilibrium frequency of sequence $\boldsymbol{\nu}$ in a mutational process, $M_{\boldsymbol{\mu\nu}}$. The mutation rate per population is equal to $2NM_{\boldsymbol{\mu\nu}}$ for a duploid population, where N is the population size. The substitution rate is equal to the product of the mutation rate and the fixation rate.

$$R_{\boldsymbol{\mu\nu}} \quad = \quad 2NM_{\boldsymbol{\mu\nu}} u(s(\boldsymbol{\mu} \to \boldsymbol{\nu})) \tag{7}$$

where $u(s(\boldsymbol{\mu} \to \boldsymbol{\nu}))$ is the fixation probability of mutants from $\boldsymbol{\mu}$ to $\boldsymbol{\nu}$ the selective advantage of which is equal to s.

In a duploid population, the fixation probability, u, of a mutant, the selective advantage of which is equal to s and the frequency of which in a population is equal to q_m, was estimated (18) as

$$2Nu(s) \quad = \quad 2N \frac{1 - e^{-4N_e s q_m}}{1 - e^{-4N_e s}} \tag{8}$$

$$= \quad \frac{u(s)}{u(0)} \qquad \text{with} \qquad q_{\rm m} = \frac{1}{2N} \qquad \text{for duploid} \tag{9}$$

where N_e is an effective population size. The selective advantage of a mutant sequence $\boldsymbol{\nu}$ to a wildtype $\boldsymbol{\mu}$ is equal to

$$s(\boldsymbol{\mu} \to \boldsymbol{\nu}) \quad = \quad m(\boldsymbol{\nu}) - m(\boldsymbol{\mu}) \tag{10}$$

where $m(\boldsymbol{\nu})$ is the Malthusian fitness of a mutant sequence, and $m(\boldsymbol{\mu})$ is for the wildtype.

This Markov process of substitutions in sequence is reversible, and the equilibrium frequency, $P^{\rm eq}(\boldsymbol{\mu})$, for each sequence is represented by

$$P^{\rm eq}(\boldsymbol{\mu}) \quad = \quad \frac{P^{\rm mut}(\boldsymbol{\mu}) \exp(4N_e m(\boldsymbol{\mu})(1 - q_m))}{\sum_{\boldsymbol{\nu}} P^{\rm mut}(\boldsymbol{\nu}) \exp(4N_e m(\boldsymbol{\nu})(1 - q_m))} \tag{11}$$

because both the mutation and fixation processes satisfy the detailed balance conditions, Eq. 6 and the following equation, respectively.

$$\exp(4N_e m(\boldsymbol{\mu})(1 - q_m)) u(s(\boldsymbol{\mu} \to \boldsymbol{\nu}))$$

$$= \quad \frac{\exp(-4N_e m(\boldsymbol{\mu}) q_m) - \exp(-4N_e m(\boldsymbol{\nu}) q_m)}{\exp(-4N_e m(\boldsymbol{\mu})) - \exp(-4N_e m(\boldsymbol{\nu}))} \tag{12}$$

$$= \quad \exp(4N_e m(\boldsymbol{\nu})(1 - q_m)) u(s(\boldsymbol{\nu} \to \boldsymbol{\mu})) \tag{13}$$

As a result, the ensemble of homologous sequences in molecular evolution obeys a Boltzmann distribution.

1.2 Relationships between $m(\boldsymbol{\sigma})$, $\psi_N(\boldsymbol{\sigma})$, and $\Delta G_{ND}(\boldsymbol{\sigma})$ of protein sequence

From Eqs. S1, S17, S18, and 11 , we can get the following relationships among the Malthusian fitness m, the folding free energy change ΔG_{ND} and $\Delta\psi_{ND}$ of protein sequence.

$$P^{\rm eq}(\boldsymbol{\mu}) = \frac{P^{\rm mut}(\boldsymbol{\mu})\exp(4N_e m(\boldsymbol{\mu})(1-q_m))}{\sum_\nu P^{\rm mut}(\boldsymbol{\nu})\exp(4N_e m(\boldsymbol{\nu})(1-q_m)))} \tag{14}$$

$$= \frac{P^{\rm mut}(\boldsymbol{\mu})\exp(-\Delta G_{ND}(\boldsymbol{\mu},T)/(k_B T_s))}{\sum_\nu P^{\rm mut}(\boldsymbol{\nu})\exp(-\Delta G_{ND}(\boldsymbol{\nu},T)/(k_B T_s))} \tag{15}$$

$$= \frac{P^{\rm mut}(\boldsymbol{\mu})\exp(-\Delta\psi_{ND}(\boldsymbol{\mu}))}{\sum_{\boldsymbol{\nu}} P^{\rm mut}(\boldsymbol{\mu})\exp(-\Delta\psi_{ND}(\boldsymbol{\nu}))} \tag{16}$$

Then, the following relationships are derived.

$$4N_e m(\boldsymbol{\mu})(1-q_m)$$

$$= \frac{-\Delta G_{ND}(\boldsymbol{\mu},T)}{k_B T_s} + \text{constant} \tag{17}$$

$$= -\Delta\psi_{ND}(\boldsymbol{\mu},T) + \text{constant} \tag{18}$$

Selective advantage is

$$4N_e s(\boldsymbol{\mu}\to\boldsymbol{\nu})(1-q_m) = (4N_e m(\boldsymbol{\nu}) - 4N_e m(\boldsymbol{\mu}))(1-q_m) \tag{19}$$

$$= -(\Delta G_{ND}(\boldsymbol{\nu},T) - \Delta G_{ND}(\boldsymbol{\mu},T))/(k_B T_s) \tag{20}$$

$$= -(\Delta\psi_{ND}(\boldsymbol{\nu},T) - \Delta\psi_{ND}(\boldsymbol{\mu},T)) \tag{21}$$

$$= -(G_N(\boldsymbol{\nu}) - G_N(\boldsymbol{\mu}))/(k_B T_s) = -(\psi_N(\boldsymbol{\nu}) - \psi_N(\boldsymbol{\mu})) \qquad \text{if } \boldsymbol{f}(\boldsymbol{\mu}) = \boldsymbol{f}(\boldsymbol{\nu}) \tag{22}$$

2 Materials

2.1 Sequence data

We study the single domains of 8 Pfam (19) families and both the single domains and multi-domains from 3 Pfam families. In Table S1 in the Supporting Material, their Pfam ID for a multiple sequence alignment, and Uniprot ID and PDB ID with the starting- and ending-residue positions of the domains are listed. The full alignments for their families at the Pfam are used to estimate one-body interactions h and pairwise interactions J with the DCA program from "http://dca.rice.edu/portal/dca/home" (4, 5). To estimate the sample ($\overline{\psi_N}$) and ensemble ($\langle\psi_N\rangle_{\boldsymbol{\sigma}}$) averages of the total interaction, M unique sequences with no deletion are used. In order to reduce phylogenetic biases in the set of homologous sequences, we employ a sample weight ($w_{\boldsymbol{\sigma}_N}$) for each sequence, which is equal to the inverse of the number of sequences that are less than 20% different from a given sequence in a given set of homologous sequences. Only representatives of unique sequences with no deletion, which are at least 20% different from each other, are used to calculate the changes of the total interaction ($\Delta\psi_N$) due to single nucleotide nonsynonymous substitutions; the number of the representatives is almost equal to $M_{\rm eff}$ in Table S1.

3 Results

3.1 The equilibrium value of ψ_N in a fixation process of amino acid substitutions

Let us consider a fixation process of amino acid substitutions in a monoclonal approximation, in which protein evolution is assumed to proceed with single amino acid substitutions fixed at a time in a population. In this approximation, $\Delta\psi_{ND}$ and ψ_N are stationary and the ensemble of proteins attains to the equilibrium state, when the average of $\Delta\Delta\psi_{ND} \simeq \Delta\psi_N$ over singe nucleotide nonsynonymous mutations fixed in a population is equal to zero; an amino acid composition is assumed to be constant in protein evolution.

$$\langle\Delta\Delta\psi_{ND}\rangle_{\rm fixed} \simeq \langle\Delta\psi_N\rangle_{\rm fixed} = 0 \iff \Delta\psi_{ND} \text{ and } \psi_N \text{ are stationary.} \tag{23}$$

Let us use $\psi_N^{\rm eq}$ to denote the equilibrium value of ψ_N.

The average of $\Delta\psi_N$ in fixed mutants, $\langle\Delta\psi_N\rangle_{\rm fixed}$, can be calculated numerically with the probability density function (PDF) of $\Delta\Delta\psi_{ND}(\simeq\Delta\psi_N)$ for single nucleotide nonsynonymous mutations,

$$p(\Delta\Delta\psi_{ND,\rm fixed}) = p(\Delta\Delta\psi_{ND})u(s(\Delta\Delta\psi_{ND}))/\langle u(s(\Delta\Delta\psi_{ND}))\rangle \quad (24)$$

$$\simeq p(\Delta\psi_N)u(s(\Delta\psi_N))/\langle u(s(\Delta\psi_N))\rangle \quad (25)$$

where $p(\Delta\Delta\psi_{ND})$ and $p(\Delta\Delta\psi_{ND,\rm fixed})$ are the PDFs of $\Delta\Delta\psi_{ND}$ in all the arising mutants and in their fixed mutants, respectively, and $\langle u(s(\Delta\Delta\psi_{ND}))\rangle$ is the average of fixation probabilities $u(s)$ over all the mutants; see Eq. 8 for the formula of fixation probability and Eq. S88 for details. $N = 10^6$ is employed.

In the estimation of ψ_N, one-body (h) and pairwise residue-residue (J) interactions calculated by the DCA program (4, 5) are converted into the simple gauge (11), and then pairwise (J) interactions were cutoff at a certain distance to reduce noise in the estimates of J, according to Morcos et al. (20).

$$\hat{J}_{ij}(a_k,a_l) = J^{\rm s}_{ij}(a_k,a_l)H(r_{\rm cutoff}-r_{ij}) \quad (26)$$

where $J^{\rm s}$ is the statistical estimate of J in the simple gauge, H is the Heaviside step function, and r_{ij} is the distance between the centers of amino acid side chains in protein structure, and $r_{\rm cutoff}$ is a distance threshold for residue pairwise interactions; see the preceding paper (11) or the Supporting Material for details.

The PDF of $\Delta\Delta G_{ND}$ were approximated with a normal distribution (21) or a bi-normal distribution (22). Fig. 1, however, shows that a single normal distribution with the observed mean and standard deviation cannot well reproduce the observed distribution of $\Delta\psi_N$ due to single nucleotide nonsynonymous mutations. For simplicity, a log-normal distribution, $\ln\mathcal{N}(x;\mu,\sigma)$, for which x,μ and σ defined as follows, is arbitrarily used here to better reproduce observed distributions of $\Delta\psi_N$, particularly in the domain of $\Delta\psi_N < \overline{\Delta\psi_N}$, although other distributions such as inverse Γ distributions can equally well reproduce the observed ones, too.

$$p(\Delta\psi_N) \approx \ln\mathcal{N}(x;\mu,\sigma) \equiv \frac{1}{x}\mathcal{N}(\ln x;\mu,\sigma) \quad (27)$$

$$x \equiv \max(\Delta\psi_N - \Delta\psi_N^{\rm o}, 0) \quad (28)$$

$$\exp(\mu+\sigma^2/2) = \overline{\Delta\psi_N} - \Delta\psi_N^{\rm o} \quad (29)$$

$$\exp(2\mu+\sigma^2)(\exp(\sigma^2)-1) = \overline{(\Delta\psi_N - \overline{\Delta\psi_N})^2)} \quad (30)$$

$$\Delta\psi_N^{\rm o} \equiv \min(\overline{\Delta\psi_N} - n_{\rm shift}\overline{(\Delta\psi_N - \overline{\Delta\psi_N})^2)}^{1/2}, 0) \quad (31)$$

where $\Delta\psi_N^{\rm o}$ is the origin for the log-normal distribution and the shifting factor $n_{\rm shift}$ is taken to be equal to 2, unless specified. Fig. 1 shows that log-normal distributions can better reproduce the observed distribution of $\Delta\psi_N$ due to single nucleotide nonsynonymous mutations except in the tails. Disagreements between the log-normal and observed distributions in the domain of $\Delta\psi_N > \overline{\Delta\psi_N}$ do not much affect the PDF of $\Delta\psi_N$ in fixed mutants, because fixation probabilities for $\Delta\psi_N(> \overline{\Delta\psi_N})$ are too low.

The average of $\Delta\psi_N$ over fixed mutants is uniquely determined by the distribution of $\Delta\Delta\psi_N(\simeq\Delta\psi_N)$, which is approximated here by a log-normal distribution estimated from the mean and variance of $\Delta\psi_N$; it depends also on q_m, which is assumed to be constant, through fixation probability, because $2N_e s \simeq -\Delta\psi_N/(1-q_m)$. In other words, $\langle\Delta\psi_N\rangle_{\rm fixed}$ is uniquely determined by the mean and variance of $\Delta\psi_N$. Therefore, under the equilibrium condition $\langle\Delta\psi_N\rangle_{\rm fixed} = 0$, only one of the mean and variance can be freely specified, and the other is uniquely determined. We employ $\overline{\Delta\psi_N}$ or ψ_N as a parameter, because $\overline{\Delta\psi_N}$ depends on ψ_N, and only one of them can be specified. We define $\overline{\Delta\psi_N}^{\rm eq}$ as $\overline{\Delta\psi_N}$ at which $\langle\Delta\psi_N\rangle_{\rm fixed} = 0$.

Suppose that the regression equation, Eq. 1, of $\Delta\psi_N$ on ψ_N is exact, and the variance of $\Delta\psi_N$ is constant irrespective of ψ_N; the slope (α_{ψ_N}), $\overline{\Delta\psi_N}$, $\overline{\rm Var(\Delta\psi_N)}$, and $\overline{\psi_N}$ that are estimated with $r_{\rm cutoff}\sim 8$Å for the PDZ and listed in Table S2 are employed here. In Fig. 2, the average of $\Delta\psi_N$ over single nucleotide nonsynonymous substitutions fixed in a population, $\langle\Delta\psi_N\rangle_{\rm fixed}$, is plotted against ψ_N/L of a wildtype for the PDZ protein family. This figure shows that $\langle\Delta\psi_N\rangle_{\rm fixed}$ changes its value from positive to negative as ψ_N increases, that is, the value of ψ_N at which $\langle\Delta\psi_N\rangle_{\rm fixed} = 0$, $\psi_N^{\rm eq}$, is the stable equilibrium value for ψ_N. In order for protein to have such a stable equilibrium value for folding free energy ($\Delta G_{ND} = k_B T_s \Delta\psi_{ND}$), the regression coefficient of $\overline{\Delta\psi_N}$ on ψ_N must be more negative than that of the standard deviation (Sd($\Delta\psi_N$)). This condition is, of course, satisfied for all protein families studied here, because the mean of $\Delta\psi_N$ over all substitutions at all sites is negatively proportional to ψ_N of a wildtype, but its standard deviation is nealy constant irrespective of ψ_N across homologous sequences; see Tables S2 and S5.

The equilibrium value $\psi_N^{\rm eq}$ is very close to the average of ψ_N over homologous proteins in the PDZ family, indicating that the present methods for a fixation process of amino acid substitutions and for the equilibrium ensemble of ψ_N give a consistent result with each other. The equilibrium value of ψ_N for each protein domain with the estimated values of α_{ψ_N}, $\overline{\psi_N}$, $\overline{\overline{\Delta\psi_N}}$, and $\overline{\mathrm{Var}(\Delta\psi_N)}$ listed in Tables S2 and S5 is calculated on the basis of the monoclonal approximation. In Fig. 3, the equilibrium values of ψ_N/L estimated with $n_{\rm shift} = 1.5, 2$, and 2.5 in the monoclonal approximation are plotted against the average of ψ_N/L over homologous sequences for each protein family. The agreement between the time average ($\psi_N^{\rm eq}$) and ensemble average ($\langle\psi_N\rangle_\sigma (= \overline{\psi_N})$) is better for $r_{\rm cutoff} \sim 8$Å than for $r_{\rm cutoff} \sim 15.5$Å and is not bad in the case of $r_{\rm cutoff} \sim 8$Å , confirming that it is a good approximation to assume the variance of $\Delta\psi_N$ not to depend on ψ_N.

3.2 Relationships between $\overline{\Delta\psi_N}(= \overline{\Delta\psi_N}^{eq})$ and the standard deviation of $\Delta\psi_N$, $\hat{T}_s$, and $\Delta\Delta\hat{G}_{ND}$ at equilibrium

In the present model, the equilibrium values, $\psi_N^{\rm eq}$ and the corresponding $\overline{\Delta\psi_N}^{\rm eq}$, are functions of the mean and variance of $\Delta\psi_N$ only, because the distribution of $\Delta\Delta\psi_{ND} (\simeq \Delta\psi_N)$ is approximately estimated with the mean and variance of $\Delta\psi_N$. On the other hand, $\psi_N^{\rm eq}$ and $\overline{\Delta\psi_N}^{\rm eq}$ should be equal to $\overline{\psi_N} = \langle\psi_N\rangle$ and $\overline{\overline{\Delta\psi_N}}$, respectively; the time average and ensemble average should be consistent. Actually $\psi_N^{\rm eq}$ almost agrees with $\overline{\psi_N}$ as shown in Fig. 3. Therefore the variance of $\Delta\psi_N$ is uniquely determined from their mean as long as ψ_N and $\overline{\Delta\psi_N}$ are at equilibrium; conversely the equilibrium value of $\overline{\Delta\psi_N}$ is determined by the variance. In Fig. 4, the standard deviation of $\Delta\psi_N$ is plotted against $\overline{\Delta\psi_N} (= \overline{\Delta\psi_N}^{\rm eq})$. Likewise the estimate of effective temperature of selection ($\hat{T}_s$) and that of folding free energy change ($\Delta\Delta\hat{G}_{ND}$) are plotted as a function of $\overline{\Delta\psi_N} (= \overline{\Delta\psi_N}^{\rm eq})$ in Figs. 5. These figures show that the averages, $\overline{\overline{\Delta\psi_N}}$ and $\overline{\mathrm{Var}(\psi_N)}^{1/2}$, over homologous sequences scatter along the curves.

3.3 Protein evolution at equilibrium, $\langle\Delta\psi_N\rangle_{fixed} = 0$

Let us consider the distributions of $\Delta\psi_N$ and K_a/K_s at equilibrium, $\langle\Delta\psi_N\rangle_{\rm fixed} = 0$; K_a/K_s is the ratio of nonsynonymous to synonymous substitution rate per site (23) and defined here as $K_a/K_s \equiv u(s)/u(0)$, where $u(s)$ is a fixation probability for selective advantage s; see Eq. S85. Fig. 6 shows the PDFs of $\Delta\psi_N$ in all single nucleotide nonsynonymous mutations and in their fixed mutations as a function of $\overline{\Delta\psi_N} (= \overline{\Delta\psi_N}^{\rm eq})$, respectively. Because $4N_e s(1-q_m) = -\Delta\Delta\psi_{ND} \simeq -\Delta\psi_N$, the PDFs of $\Delta\psi_N$ can be regarded as the PDFs of $4N_e s(1-q_m)$. At equilibrium, the distribution of $\Delta\psi_N$ in all single nucleotide nonsynonymous mutants becomes wider as the mean of $\Delta\psi_N$ increases, however, that in fixed mutants remains to be narrow with a peak near zero.

The common understanding of protein evolution has been that amino acid substitutions observed in homologous proteins are neutral (12–15) or slightly deleterious (16, 17), and random drift is a primary force to fix amino acid substitutions in population. In order to see how significant neutral/slightly deleterious substitutions are in protein evolution, the PDFs of K_a/K_s in all single nucleotide nonsynonymous mutations and in their fixed mutations are calculated, and shown in Fig. 6. The blue line on the landscape of the PDF shows the averages of K_a/K_s. The averages of K_a/K_s in all single nucleotide nonsynonymous mutations and in their fixed mutations are also shown in Fig. 7. The average of K_a/K_s in all the arising mutants is less than 1 and decreases as $\overline{\Delta\psi_N} \simeq \overline{\Delta\psi_N}^{\rm eq}$ increases, indicating that negative mutants significantly occur and increase as $\overline{\Delta\psi_N}$ increases. On the other hand, $\langle K_a/K_s\rangle_{\rm fixed}$ in fixed mutants is larger than 1 and increases as $\Delta\psi_N^{\rm eq}$ increases, indicating that positive mutants fix significantly in population and increase as equilibrium folding free energy change increases, that is, equilibrium protein stability decreases. To see each contribution of positive, neutral, slightly negative and negative selections, the value of K_a/K_s is divided arbitrarily into four categories, $K_a/K_s > 1.05$, $1.05 > K_a/K_s > 0.95$, $0.95 > K_a/K_s > 0.5$, and $0.5 > K_a/K_s$ for their selection categories, respectively. The probabilities of each selection category in all single nucleotide nonsynonymous mutations and their fixed mutations are shown in Fig. 8, respectively. Stabilizing mutations are significantly fixed by positive selection, and balance with destabilizing mutations fixed by random drift. Of course, most destabilizing mutations in slightly negative and negative selection categories are removed from population. Surprisingly, the proportion of neutral selection is not large even in fixed mutations.

3.4 Relationship between T_s and K_a/K_s

As the effective temperature of selection (T_s) decreases, the total interaction ($\langle\psi_N(\boldsymbol{\sigma})\rangle_\sigma$) of a protein decreases and the change of interaction ($\overline{\Delta\psi_N}^{\rm eq}$) due to single amino acid substitutions increases; see Fig. 5. Thus, destabilizing mutations increase, and an amino acid substitution rate is expected to decrease. Fig. 7 shows that the average of K_a/K_s decreases as $\overline{\Delta\psi_N}^{\rm eq}$ increases.

The direct relationship between substitution rate and T_s is shown in Fig. 9; the average of K_a/K_s decreases as T_s increases. In the selection maintaining protein foldability/stability, the effective temperature of selection is directly reflected in amino acid substitution rate.

4 Discussion

A purpose of the present study is to formulate protein fitness originating in protein foldability and stability. From a phenomenological viewpoint, Drummond and Wilke (24) took notice of toxicity of misfolded proteins as well as diversion of protein synthesis resources, and formulated a Malthusian fitness of a genome to be negatively proportional to the total amount of misfolded proteins, which must be produced to obtain the necessary amount of folded proteins (21). They also formulated a Malthusian fitness based on protein dispensability to be negatively proportional to the ratio of unfolded proteins. These formulas of protein fitness can be well approximated by a generic form, $m = -\kappa \exp(\Delta G_{ND}/(k_B T))$, where T is a growth temperature, and $\kappa(\geq 0)$ is a parameter, which depends on protein disability and cellular abundance of protein (25).

On the other hand, the present formulas for protein fitness, Eqs. 17 and 18 , have been derived on the basis of a protein folding theory, particularly the random energy model, and the maximum entropy principle for the distribution of homologous sequences in sequence space. The former indicates that the equilibrium ensemble of sequences is a canonical ensemble with the Boltzmann factor $\exp(-\Delta G_{ND}/k_B T_s)$, and the latter insists that the probability distribution of homologous sequences, which satisfies a given amino acid composition at each site and a given pairwise amino acid frequency at each site pair, can be represented as a Boltzmann distribution with $\exp(-\psi_N)$, in which the total interaction (ψ_N) is represented as the sum of one-body and pairwise interactions between sites. On the other hand, assuming mutation and fixation processes to be reversible Markov processes leads us to a formulation that the equilibrium ensemble of sequences also obeys a Boltzmann distribution with $\exp(4N_e m(1-q_m))$. As a result, we obtain the correspondences between folding free energy ($-\Delta G_{ND}/k_B T_s$), and $-\Delta\psi_{ND}$ and protein fitness ($2N_e m(1-q_m)$).

In the comparison of these two formulas of protein fitness, it may be interpreted that $4N_e(1-q_m)\kappa/T \sim 1/T_s$, if $|\Delta G_{ND}/(k_B T)| << 1$, however, the growth temperature T and folding free energy do not always satisfy this condition. Selective advantage of mutant is not upper-bounded in the present scheme of a Malthusian fitness but in the case of $m = -\kappa \exp(\Delta G_{ND}/(k_B T))$. As a result, PDFs of K_a/K_s in all arising mutations and in fixed mutations have very different shapes from each other (25). The most advantage of the present fitness scheme, however, is that it reproduces the distribution of homologous sequences fixed in protein evolution. Thus, the present formula for protein fitness would better describe natural selection maintaining protein's stability and foldability over evolutionary timescales.

In the monoclonal approximation, it has been confirmed that the time average ($\psi_N^{\rm eq}$) and ensemble average ($\overline{\psi_N} = \langle\psi_N\rangle_{\boldsymbol{\sigma}}$) of the total interaction (ψ_N) almost agree with each other. The equilibrium value $\psi_N^{\rm eq}$, where the average of $\Delta\psi_N$ over fixed mutants is equal to zero, is calculated with the approximation of the distribution of $\Delta\psi_N$ by a log-normal distribution and the empirical rules of Eqs. 1 and 3. Therefore, this result also supports these approximations and empirical rules, particularly Eq. 3, that is, the constancy of the variance of $\Delta\psi_N$ irrespective of ψ_N of a wildtype. In the monoclonal approximation together with the log-normal distribution approximation, $\overline{\Delta\psi_N}^{\rm eq}$, $\mathrm{Sd}(\Delta\psi_N)^{\rm eq}$, $\hat{T}_s$, and $\Delta\Delta\hat{G}_{ND}$ can been determined as a function of any one of them. Here they have been shown as a function of $\overline{\Delta\psi_N}^{\rm eq}$.

We also study the evolution of protein at equilibrium, at which the ensemble of homologous sequences obeys a Boltzmann distribution with $\exp(-\Delta G_{ND}/(k_B T_s))$, and the ensemble averages of the native conformational free energy $G_N(= k_B T_s \psi_N)$ and folding free energy change $\Delta\Delta G_{ND}(= k_B T_s \Delta\Delta\psi_{ND} \simeq k_B T_s \Delta\psi_N)$ agree with their stationary values; $\langle\psi_N\rangle_{\boldsymbol{\sigma}} = \overline{\psi_N} = \psi_N^{\rm eq}$ and $\langle\overline{\Delta\psi_N}\rangle\boldsymbol{\sigma} = \overline{\overline{\Delta\psi_N}} = \overline{\Delta\psi}_N^{\rm eq}$. Approximating the PDF of $\Delta\psi_N$ due to single nucleotide nonsynonymous substitutions by a log-normal distribution, the PDFs of $\Delta\psi_N$ and K_a/K_s in all the mutants and in their fixed mutants have been estimated. It is confirmed that the effective temperature (T_s) of selection negatively correlates with the amino acid substitution rate (K_a/K_s) of protein. Interestingly, stabilizing mutations are significantly fixed in population by positive selection, and balance with destabilizing mutations that are also significantly fixed by random drift, although most negative mutations are removed from population. This is clear, because at equilibrium the average of K_a/K_s in all the mutants is less than 1, but that in their fixed mutants is larger than 1. Contrary to the neutral theory (12–15), the proportion of neutral selection is not large even in fixed mutants. It should be noted that these conclusions based on the PDFs of $\Delta\psi_N$ and K_s/K_s require only an equilibrium condition of $\overline{\Delta\psi_N} = \overline{\Delta\psi}_N^{\rm eq}$, but does not require the approximation of constancy for the variance of ΔG_N, which is used only to estimate T_s and $\psi_N^{\rm eq}$ and other relations based on T_s.

5 Supporting Citation

References (26–43) appear in the Supporting Material.

SUPPLEMENTARY MATERIAL

An online supplement to this article can be found by visiting BJ Online at http://www.biophysj.org.

References

1. Bryngelson, J. D., and P. G. Wolynes, 1987. Spin glasses and the statistical mechanics of protein folding. Proc. Natl. Acad. Sci. USA 84:7524–7528.
2. Ramanathan, S., and E. Shakhnovich, 1994. Statistical mechanics of proteins with evolutionary selected sequences. Phys. Rev. E 50:1303–1312.
3. Pande, V. S., A. Y. Grosberg, and T. Tanaka, 1997. Statistical mechanics of simple models of protein folding and design. Biophys. J. 73:3192–3210.
4. Morcos, F., A. Pagnani, B. Lunt, A. Bertolino, D. S. Marks, C. Sander, R. Zecchina, J. N. Onuchic, T. Hwa, and M. Weigt, 2011. Direct-coupling analysis of residue coevolution captures native contacts across many protein families. Proc. Natl. Acad. Sci. USA 108:E1293–E1301.
5. Marks, D. S., L. J. Colwell, R. Sheridan, T. A. Hopf, A. Pagnani, R. Zecchina, and C. Sander, 2011. Protein 3D Structure Computed from Evolutionary Sequence Variation. PLoS ONE 6:e28766. http://dx.doi.org/10.1371/journal.pone.0028766.
6. Ekeberg, M., C. Lövkvist, Y. Lan, M. Weigt, and E. Aurell, 2013. Improved contact prediction in proteins: Using pseudolikelihoods to infer Potts models. Phys. Rev. E 87:012707–1–16. http://link.aps.org/doi/10.1103/PhysRevE.87.012707.
7. Ekeberg, M., T. Hartonen, and E. Aurell, 2014. Fast pseudolikelihood maximization for direct-coupling analysis of protein structure from many homologous amino-acid sequences. J. Comput. Phys. 276:341–356.
8. Miyazawa, S., 2013. Prediction of Contact Residue Pairs Based on Co-Substitution between Sites in Protein Structures. PLoS ONE 8:e54252. http://dx.doi.org/10.1371/journal.pone.0054252.
9. Sułkowska, J. I., F. Morcos, M. Weigt, T. Hwa, and J. N. Onuchic, 2012. Genomics-aided structure prediction. Proc. Natl. Acad. Sci. USA 109:10340–10345.
10. Hopf, T. A., L. J. Colwell, R. Sheridan, B. Rost, C. Sander, and D. S. Marks, 2012. Three-Dimensional Structures of Membrane Proteins from Genomic Sequencing. Cell 149:1607–1621.
11. Miyazawa, S., 2016. Selection originating from protein foldability: A new method to estimate selection temperature .
12. Kimura, M., 1968. Evolutionary rate at the molecular level. Nature 217:624–626.
13. Kimura, M., 1969. The rate of molecular evolution considered from the standpoint of population genetics. Proc. Natl. Acad. Sci. USA 63:1181–1188.
14. Kimura, M., and T. Ohta, 1971. Protein Polymorphism as a Phase of Molecular Evolution. Nature 229:467–469.
15. Kimura, M., and T. Ohta, 1974. On some principles governing molecular evolution. Proc. Natl. Acad. Sci. USA 71:2848–2852.
16. Ohta, T., 1973. Slightly Deleterious Mutant Substitutions in Evolution. Nature 246:96–98.
17. Ohta, T., 1992. The nearly neutral theory of molecular evolution. Annu. Rev. Ecol. Syst. 23:263–286.
18. Crow, J. F., and M. Kimura, 1970. An Introduction to population genetics theory. Harper & Row publishers, New York.
19. Finn, R., P. Coggill, R. Y. Eberhardt, S. R. Eddy, J. Mistry, A. L. Mitchell, S. C. Potter, M. Punta, M. Qureshi, A. Sangrador-Vegas, G. A. Salazar, and A. B. J. Tate, 2016. The Pfam protein families database; towards a more sustainable future. Nucl. Acid Res. 44:D279–D285.
20. Morcos, F., N. P. Schafer, R. R. Cheng, J. N. Onuchic, and P. G. Wolynes, 2014. Coevolutionary information, protein folding landscapes, and the thermodynamics of natural selection. Proc. Natl. Acad. Sci. USA 111:12408–12413.
21. Serohijos, A., Z. Rimas, and E. Shakhnovich, 2012. Protein Biophysics Explains Why Highly Abundant Proteins Evolve Slowly. Cell Reports 2:249 – 256. http://dx.doi.org/10.1016/j.celrep.2012.06.022.
22. Tokuriki, N., F. Stricher, J. Schymkowitz, L. Serrano, and D. S. Tawfik, 2007. The Stability Effects of Protein Mutations Appear to be Universally Distributed. J. Mol. Biol. 369:1318–1332.
23. Miyata, T., and T. Yasunaga, 1980. Molecular evolution of mRNA: a method for estimating evolutionary rates of synonymous and amino acid substitutions from homologous nucleotide sequences and its applications. J. Mol. Evol. 16:23–36.
24. Drummond, D. A., and C. O. Wilke, 2008. Mistranslation-Induced Protein Misfolding as a Dominant Constraint on Coding-Sequence Evolution. Cell 134:341 – 352. http://dx.doi.org/10.1016/j.cell.2008.05.042.
25. Miyazawa, S., 2016. Selection maintaining protein stability at equilibrium. J. Theor. Biol. 391:21–34.
26. Gianni, S., C. D. Geierhaas, N. Calosci, P. Jemth, G. W. Vuister, C. Travaglini-Allocatelli, M. Vendruscolo, and M. Brunori, 2007. A PDZ domain recapitulates a unifying mechanism for protein folding. Proc. Natl. Acad. Sci. USA 104:128–133.
27. Rosa, C. L., D. Milardi, D. Grasso, R. Guzzi, and L. Sportelli, 1995. Thermodynamics of the Thermal Unfolding of Azurin. J. Phys. Chem. 99:14864–14870.
28. Ganguly, T., M. Das, A. Bandhu, P. K. Chanda, B. Jana, R. Mondal, and S. Sau, 2009. Physicochemical properties and distinct DNA

binding capacity of the repressor of temperate Staphylococcus aureus phage ϕ/11. FEBS J. 276:1975–1985.

29. Ruiz-Sanz, J., A. Simoncsits, I. Tőrő, S. Pongor, P. L. Mateo, and V. V. Filimonov, 1999. A thermodynamic study of the 434-repressor N-terminal domain and of its covalently linked dimers. Eur. J. Biochem 263:246–253.
30. Stupák, M., G. Zŏldák, A. Musatov, M. Sprinzl, and E. Sedlák, 2006. Unusual effect of salts on the homodimeric structure of NADH oxidase from *Thermus thermophilus* in acidic pH. Biochim. Biophys. Acta 1764:129–137.
31. D'Auria, S., A. Scirè, A. Varriale, V. Scognamiglio, M. Staiano, A. Ausili, A. Marabotti, MosèRossi, and F. Tanfani, 2005. Binding of Glutamine to Glutamine-Binding Protein from *Escherichia coli* Induces Changes in Protein Structure and Increases Protein Stability. Proteins 58:80–87.
32. Parsons, L. M., F. Lin, and J. Orban, 2006. Peptidoglycan Recognition by Pal, an Outer Membrane Lipoprotein. Biochemistry 45:2122–2128.
33. Williams, N. K., P. Prosselkov, E. Liepinsh, I. Line, A. Sharipo, D. R. Littler, P. M. G. Curmi, G. Otting, and N. E. Dixon, 2002. *In Vivo* Protein Cyclization Promoted by a Circularly Permuted *Synechocystis* sp. PCC6803 DnaB Mini-intein. J. Biol. Chem. 277:7790–7798.
34. Sainsbury, S., J. Ren, N. J. Saunders, D. I. Stuarta, and R. J. Owens, 2008. Crystallization and preliminary X-ray analysis of CrgA, a LysR-type transcriptional regulator from pathogenic *Neisseria meningitidis* MC58. Acta Cryst. F64:797–801.
35. Armengaud, J., J. Urbonavicius, B. Fernandez, G. Chaussinand, J. M. Bujnicki, and H. Grosjean, 2004. N^2-Methylation of Guanosine at Position 10 in tRNA Is Catalyzed by a THUMP Domain-containing, S-Adenosylmethionine-dependent Methyltransferase, Conserved in Archaea and Eukaryota. JBiolChem 279:37142–37152.
36. Guelorget, A., M. Roovers, V. Guérineau, C. Barbey, X. Li, , and B. Golinelli-Pimpaneau, 2010. Insights into the hyperthermostability and unusual region-specificity of archaeal *Pyrococcus abyssi* tRNA m^1A57/58 methyltransferase. Nucl. Acid Res. 38:6206–6218.
37. Knapp, S., P. T. Mattson, P. Christova, K. D. Berndt, A. Karshikoff, M. Vihinen, C. E. Smith, and R. Ladenstein, 1998. Thermal Unfolding of Small Proteins With SH3 Domain Folding Pattern. Proteins 31:309–319.
38. Grantcharova, V. P., D. S. Riddle, J. V. Santiago, and D. Baker, 1998. Important role of hydrogen bonds in the structurally polarized transition state for folding of the src SH3 domain. Nature Struct. Biol 714–720.
39. Onwukwe, G. U., P. Kursula1, M. K. Koski, W. Schmitz, and R. K. Wierenga, 2014. Human Δ^3,Δ^2-enoyl-CoA isomerase, type 2: a structural enzymology study on the catalytic role of its ACBP domain and helix-10. FEBS J. 282:746–768.
40. Kragelund, B. B., P. Osmark, T. B. Neergaard, J. Schiødt, K. Kristiansen, J. Knudsen, and F. M. Poulsen, 1999. The formation of a native-like structure containing eight conserved hydrophobic residues is rate limiting in two-state protein folding of ACBP. Nature Struct. Biol 6:594–601.
41. Torchio, G. M., M. R. Ermácora, and M. P. Sica, 2012. Equilibrium Unfolding of the PDZ Domain of β2-Syntrophin. Biophys. J. 102:2835–2844.
42. Gianni, S., N. Calosci1, J. M. A. Aelen, G. W. Vuister, M. Brunori, and C. Travaglini-Allocatelli, 2005. Kinetic folding mechanism of PDZ2 from PTP-BL. Protein Eng. Design Selection 18:389–395.
43. Wilson, C. J., and P. Wittung-Stafshede, 2005. Snapshots of a Dynamic Folding Nucleus in Zinc-Substituted Pseudomonas aeruginosa Azurin. Biochemistry 44:10054–10062.

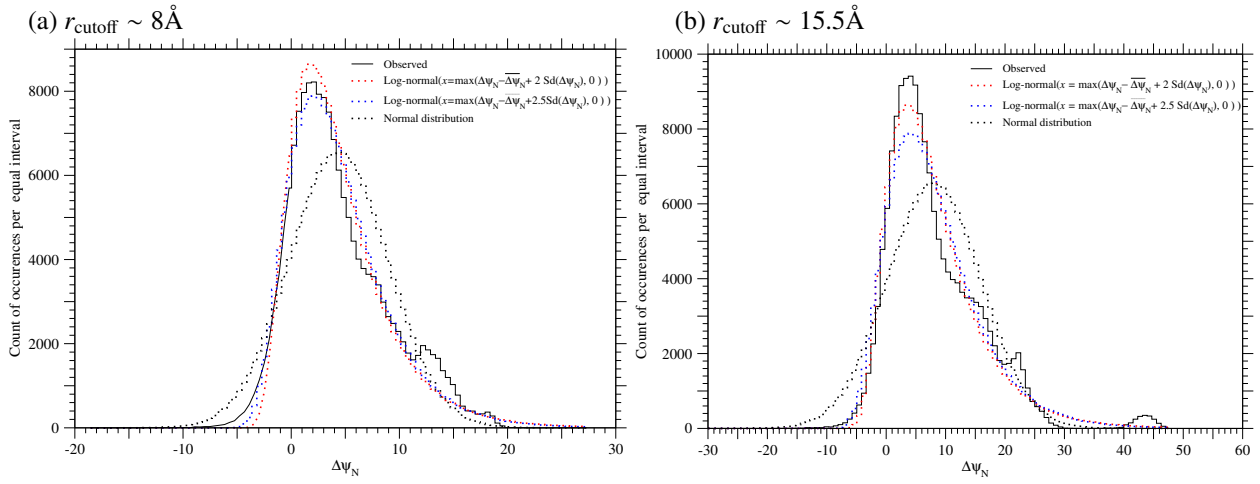
(a) r_{cutoff} ~ 8Å
Observed
Log-normal(x=max(ΔψN−ΔψN+ 2 Sd(ΔψN), 0))
Log-normal(x=max(ΔψN−ΔψN+2.5Sd(ΔψN), 0))
Normal distribution
Count of occurences per equal interval
ΔψN
(b) r_{cutoff} ~ 15.5Å
Observed
Log-normal(x = max(ΔψN− ΔψN + 2 Sd(ΔψN), 0))
Log-normal(x = max(ΔψN− ΔψN+ 2.5 Sd(ΔψN), 0))
Normal distribution
Count of occurences per equal interval
ΔψN

Figure 1: **The observed frequency distribution and the fitted distributions of $\Delta\psi_N$ in the PDZ protein family.** A black solid line indicates the observed frequency distribution of $\Delta\psi_N$ per equal interval in homologous sequences of the PDZ protein family, and red dotted and blue dotted lines indicate the total frequencies of log-normal distributions with $n_{\mathrm{shift}} = 2$ or 2.5 and parameters estimated with the mean and variance of the observed distribution for each protein; see Eqs. 27 and 31. A black dotted line indicates the total frequencies of normal distributions the mean and variance of which are equal to those of the observed distribution for each protein. Only representatives of unique sequences with no deletion, which are at least 20% different from each other, are employed; the total count is equal to 164651 over 335 homologous sequences, which is almost equal to M_{eff} in Table S1.

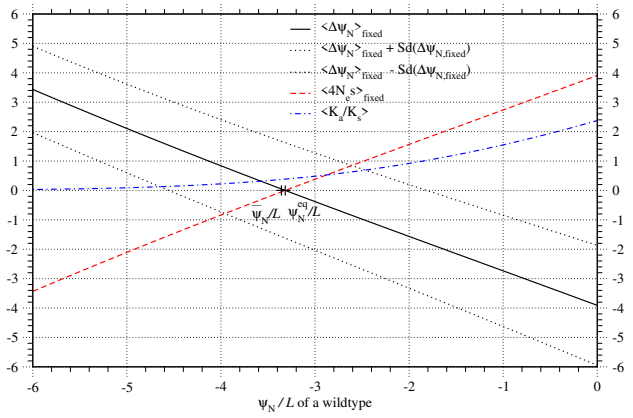

Figure 2: **The average of $\Delta\psi_N(\simeq \Delta\Delta\psi_{ND})$ over fixed single nucleotide nonsynonymous mutations versus ψ_N/L of a wildtype for the PDZ protein family.** The averages of $\Delta\psi_N(\simeq \Delta\Delta\psi_{ND})$ and $4N_e s$ over the fixed mutants, and the average of $K_a/K_s(\equiv u(s)/u(0))$ over all the mutants are plotted against ψ_N/L of a wildtype by solid, broken, and dash-dot lines, respectively; $q_m = 1/(2\times 10^6)$ is assumed. Dotted lines show the values of $\langle\Delta\psi_N\rangle_{\rm fixed} \pm$ sd, where the sd is the standard deviation of $\Delta\psi_N$ over fixed mutants. Fixation probability has been calculated in the approximation of $\Delta\Delta\psi_{ND} \simeq \Delta\psi_N$; see Eqs. 8 and 22. Here the empirical relationships of Eqs. 1 and 3 are assumed; that is, the mean of $\Delta\psi_N$ linearly decreases as ψ_N increases, but the variance of $\Delta\psi_N$ is constant irrespective of ψ_N. The slope (α_{ψ_N}) and intercept ($\overline{\overline{\Delta\psi_N}}$) and the average of the variance of $\Delta\psi_N$ over homologous sequences that are estimated with $r_{\rm cutoff} \sim 8$Å for the PDZ and listed in Table S2 are employed here. The distribution of $\Delta\psi_N$ due to single nucleotide nonsynonymous mutations is approximated by a log-normal distribution with $n_{\rm shift} = 2.0$; see Eqs. 27 and 31. The $\psi_N^{\rm eq}$, where $\langle\Delta\Delta\psi_{ND}\rangle_{\rm fixed} \simeq \langle\Delta\psi_N\rangle_{\rm fixed} = 0$, is the stable equilibrium value of ψ_N in the protein evolution of the PDZ protein family. The $\psi_N^{\rm eq}$ is close to the average of ψ_N over homologous sequences ($\overline{\psi_N}$), indicating that the present approximations for $\psi_N^{\rm eq}$ and for $\overline{\psi_N} = \langle\psi_N\rangle_{\boldsymbol{\sigma}}$ are consistent to each other.

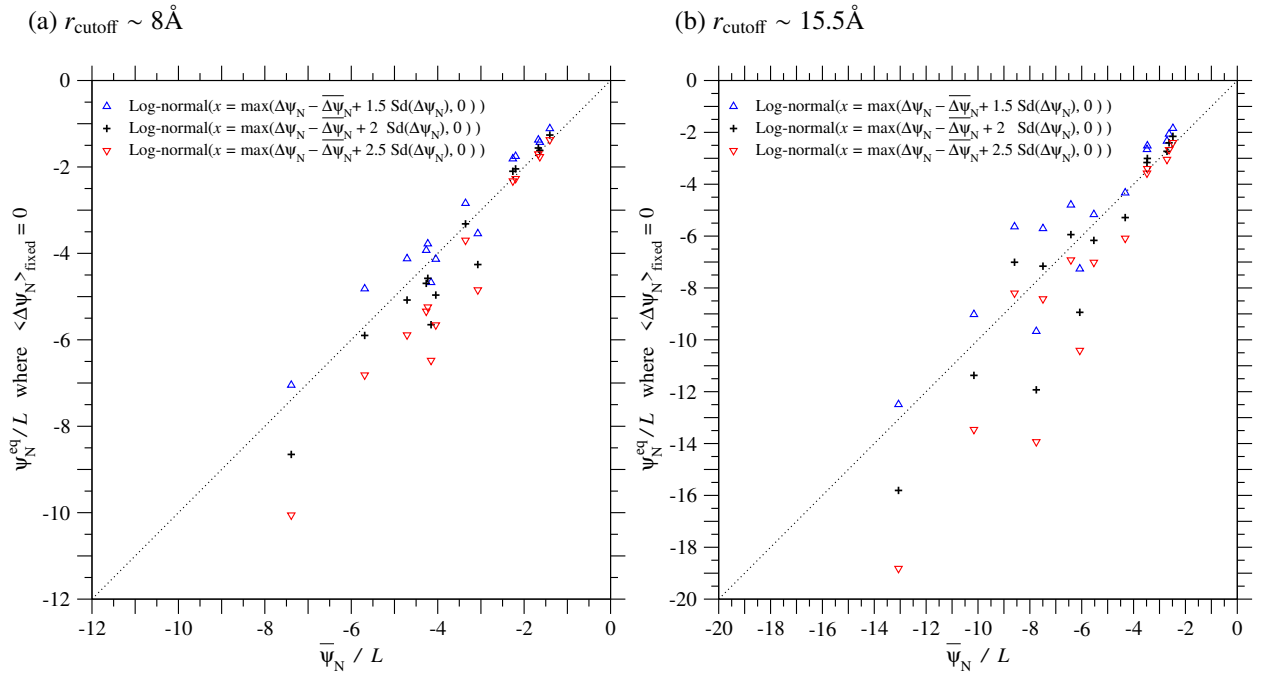
(a) $r_{\rm cutoff}$ ~ 8Å
(b) $r_{\rm cutoff}$ ~ 15.5Å
Log-normal(x = max($\Delta\psi_N - \overline{\Delta\psi_N}$+ 1.5 Sd($\Delta\psi_N$), 0))
Log-normal(x = max($\Delta\psi_N - \overline{\Delta\psi_N}$ + 2 Sd($\Delta\psi_N$), 0))
Log-normal(x = max($\Delta\psi_N - \overline{\Delta\psi_N}$+ 2.5 Sd($\Delta\psi_N$), 0))
$\psi_N^{\rm eq}/L$ where $\langle\Delta\psi_N\rangle_{\rm fixed} = 0$
$\overline{\psi_N}$ / L

Figure 3: **The equilibrium value of ψ_N/L, where $\langle\Delta\psi_N\rangle_{\rm fixed} = 0$, is plotted against the average of ψ_N/L over homologous sequences for each protein family.** The cutoff distances, (a) $r_{\rm cutoff} = 8$Å and (b) $r_{\rm cutoff} = 15.5$Å are employed to estimate ψ_N of each protein family. The equilibrium values $\psi_N^{\rm eq}$, where $\langle\Delta\psi_N\rangle_{\rm fixed} = 0$, are calculated by using the linear dependency of $\overline{\Delta\psi_N}$ on ψ_N (Eq. 1) and estimated values with $r_{\rm cutoff} \sim 8$ or 15.5Å in Tables S2 or S5. The variance of $\Delta\psi_N$ is approximated to be constant and equal to $\overline{\rm Var(\Delta\psi_N)}$; see Eq. 3. Plus, upper triangle, and lower triangle marks indicate the cases of log-normal distributions with $n_{\rm shift} = 1.5$, 2.0, and 2.5 employed to approximate the distribution of $\Delta\psi_N$, respectively; see Eqs. 27 and 31.

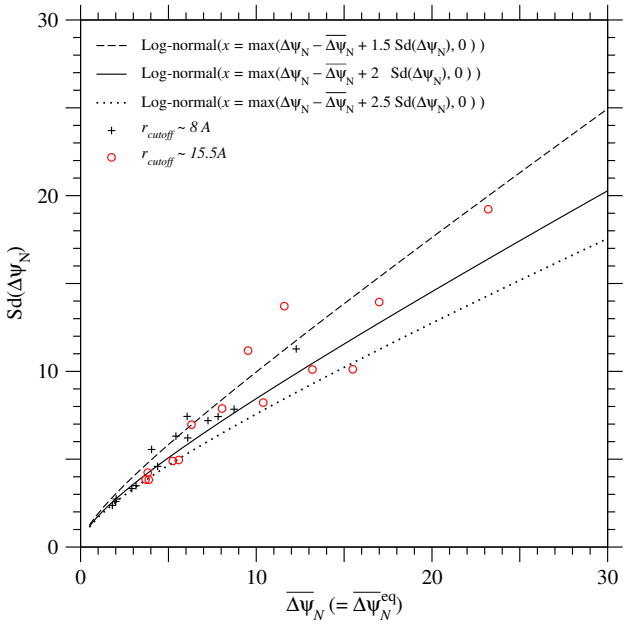
Log-normal(x = max(Δψ_N − Δψ̄_N + 1.5 Sd(Δψ_N), 0))
Log-normal(x = max(Δψ_N − Δψ̄_N + 2 Sd(Δψ_N), 0))
Log-normal(x = max(Δψ_N − Δψ̄_N + 2.5 Sd(Δψ_N), 0))
r_cutoff ~ 8 A
r_cutoff ~ 15.5A
Sd(Δψ_N)
Δψ̄_N (= Δψ̄_N^eq)
0
10
20
30

Figure 4: **Relationship between the mean and the standard deviation of $\Delta\psi_N$ due to single nucleotide nonsynonymous mutations at equilibrium,** $\langle\Delta\psi_N\rangle_{\mathbf{fixed}} = 0$ The standard deviation of $\Delta\psi_N$ that satisfies $\langle\Delta\psi_N\rangle_{\rm fixed} = 0$ is plotted against its mean, $\overline{\Delta\psi_N}$. Broken, solid, and dotted lines indicate the cases of log-normal distributions with $n_{\rm shift} = 1.5, 2.0$ and 2.5 employed to approximate the distribution of $\Delta\psi_N$, respectively; see Eqs. 27 to 31. Plus and open circle marks indicate the averages, $\overline{\overline{\Delta\psi_N}}$ and $\overline{{\rm Var}(\Delta\psi_N)}^{1/2}$, over homologous sequences in each protein family for $r_{\rm cutoff} \sim 8$ and 15.5Å, respectively; see Tables S2 and S5.

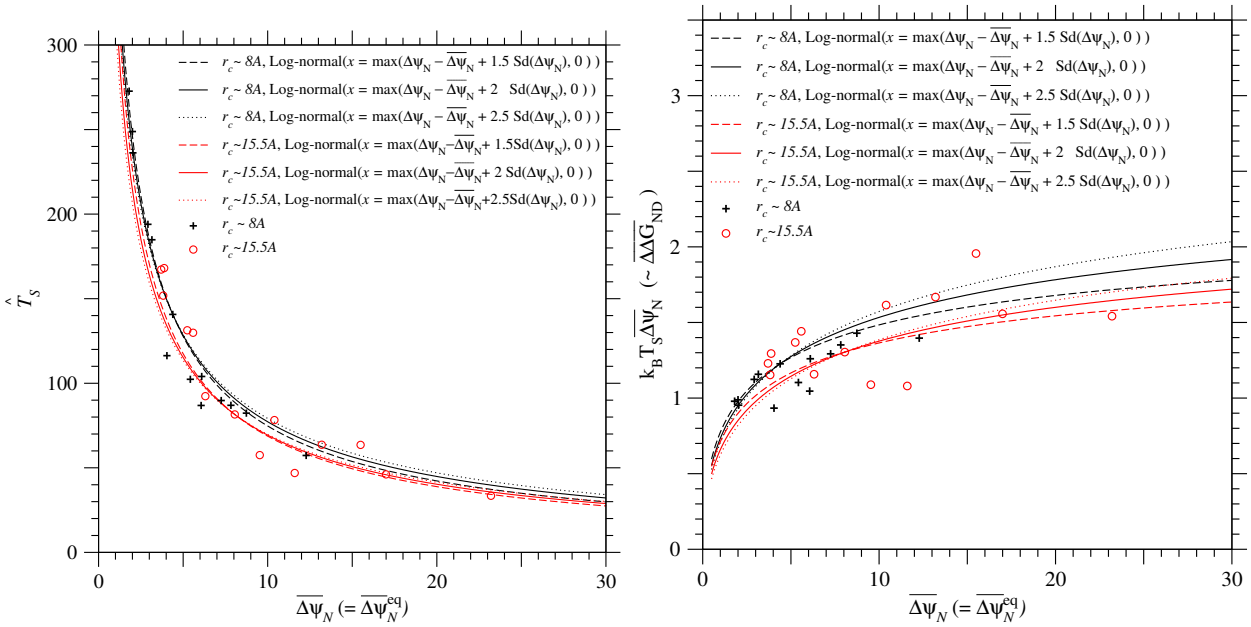
r_c~ 8A, Log-normal(x = max($\Delta\psi_N - \overline{\Delta\psi_N}$ + 1.5 Sd($\Delta\psi_N$), 0))
r_c~ 8A, Log-normal(x = max($\Delta\psi_N - \overline{\Delta\psi_N}$ + 2 Sd($\Delta\psi_N$), 0))
r_c~ 8A, Log-normal(x = max($\Delta\psi_N - \overline{\Delta\psi_N}$ + 2.5 Sd($\Delta\psi_N$), 0))
r_c~15.5A, Log-normal(x = max($\Delta\psi_N - \overline{\Delta\psi_N}$ + 1.5Sd($\Delta\psi_N$), 0))
r_c~15.5A, Log-normal(x = max($\Delta\psi_N - \overline{\Delta\psi_N}$ + 2 Sd($\Delta\psi_N$), 0))
r_c~15.5A, Log-normal(x = max($\Delta\psi_N - \overline{\Delta\psi_N}$ +2.5Sd($\Delta\psi_N$), 0))
r_c ~ 8A
r_c~15.5A
$\hat{T}_s$
$\overline{\Delta\psi_N}$ (= $\overline{\Delta\psi_N^{eq}}$)
$k_B T_s \overline{\Delta\psi_N}$ (~ $\overline{\Delta\Delta G_{ND}}$)

Figure 5: **Relationships between $\hat{T}_s$ and $\overline{\Delta\psi_N}$ and between $k_B T_s \overline{\Delta\psi_N} (\simeq \overline{\Delta\Delta\hat{G}_{ND}})$ and $\overline{\Delta\psi_N}$ at equilibrium, $\langle\Delta\psi_N\rangle_{\mathbf{fixed}} = 0$.** The estimate $\hat{T}_s$ of effective temperature for selection and the estimate of mean folding free energy change, $k_B T_s \overline{\Delta\psi_N} \simeq \overline{\Delta\Delta\hat{G}_{ND}}$, are plotted against $\overline{\Delta\psi_N}$ under the condition of $\langle\Delta\psi_N\rangle_{\text{fixed}} = 0$. The T_s is estimated in relative to the T_s of the PDZ family in the approximation (11) that the variance of ΔG_N due to single nucleotide nonsynonymous mutations is constant irrespective of protein families; see Eq. 5. Broken, solid, and dotted lines indicate the cases of log-normal distributions with $n_{\text{shift}} = 1.5, 2.0$ and 2.5 employed to approximate the distribution of $\Delta\psi_N$, respectively; see Eqs. 27 to 31. Plus and open circle marks indicate those estimates against the average of $\overline{\Delta\psi_N}$ over homologous sequences for each protein family with $r_{\text{cutoff}} \sim 8$ and 15.5Å, respectively; see Tables S2 and S5.

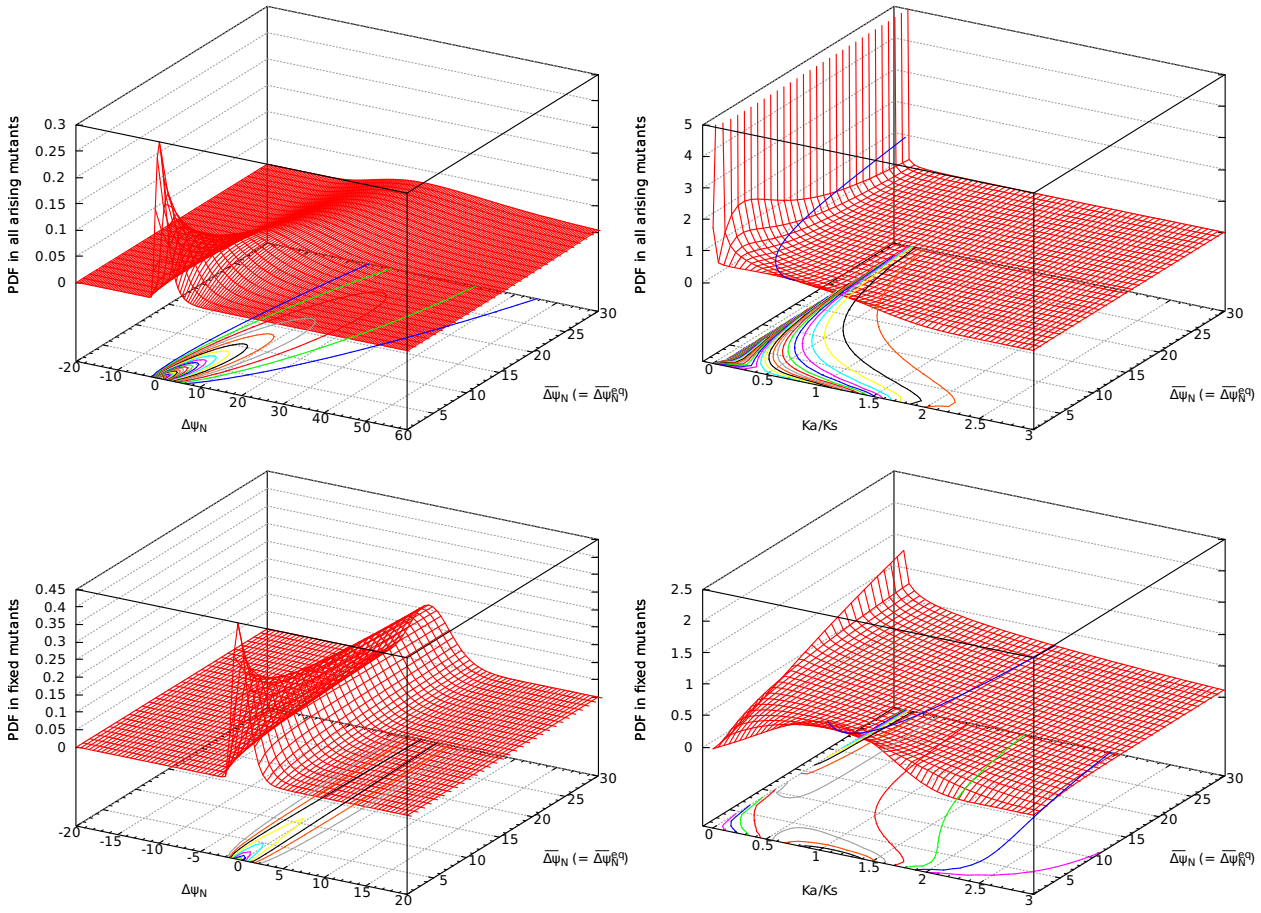

Figure 6: **PDFs of $\Delta\psi_N$ and K_a/K_s in all singe nucleotide nonsynonymous mutants and in their fixed mutants as a function of $\overline{\Delta\psi_N}$ at equilibrium, $\langle\Delta\psi_N\rangle_{\mathbf{fixed}} = 0$.** Fixation probability has been calculated in the approximation of $\Delta\Delta\psi_{ND} \simeq \Delta\psi_N$; see Eqs. 8 and 22. The distribution of $\Delta\psi_N$ due to single nucleotide nonsynonymous mutations is approximated by a log-normal distribution with $n_{\rm shift} = 2.0$; see Eqs. 27 and 31. The standard deviation of $\Delta\psi_N$ is determined to satisfy $\langle\Delta\psi_N\rangle_{\rm fixed} = 0$ at $\overline{\Delta\psi_N} = \overline{\Delta\psi_N}^{\rm eq}$.

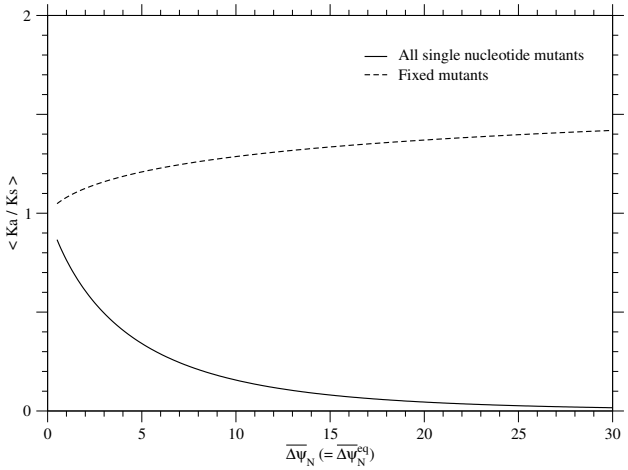

Figure 7: **The averages of K_a/Ks over all single nucleotide nonsynonymous mutations and over their fixed mutations as a function of $\overline{\Delta\psi_N}$ at equilibrium, $\langle\Delta\psi_N\rangle_{\mathbf{fixed}} = 0$.** Solid and broken lines indicate $\langle K_a/K_s\rangle$ and $\langle K_a/K_s\rangle_{\rm fixed}$, respectively. Fixation probability has been calculated in the approximation of $\Delta\Delta\psi_{ND} \simeq \Delta\psi_N$; see Eqs. 8 and 22. The distribution of $\Delta\psi_N$ due to single nucleotide nonsynonymous mutations is approximated by a log-normal distribution with $n_{\rm shift} = 2.0$; see Eqs. 27 and 31. The standard deviation of $\Delta\psi_N$ is determined to satisfy $\langle\Delta\psi_N\rangle_{\rm fixed} = 0$ at $\overline{\Delta\psi_N} = \overline{\Delta\psi_N}^{\rm eq}$.

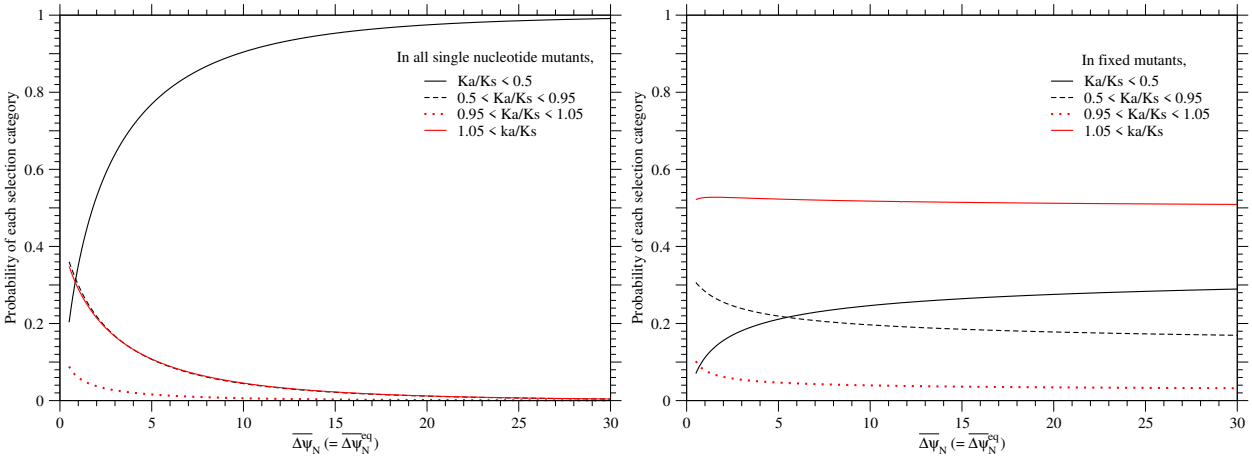
In all single nucleotide mutants,
Ka/Ks < 0.5
0.5 < Ka/Ks < 0.95
0.95 < Ka/Ks < 1.05
1.05 < ka/Ks
Probability of each selection category
In fixed mutants,
Ka/Ks < 0.5
0.5 < Ka/Ks < 0.95
0.95 < Ka/Ks < 1.05
1.05 < ka/Ks
Probability of each selection category

Figure 8: **The probabilities of each selection category in all single nucleotide nonsynonymous mutations and in their fixed mutations as a function of $\overline{\Delta\psi_N}$ at equilibrium, $\langle\Delta\psi_N\rangle_{\mathbf{fixed}} = 0$.** The left and right figures are for single nucleotide nonsynonymous mutations and for their fixed mutations, respectively. Red solid, red dotted, black broken, and black solid lines indicate positive, neutral, slightly negative and negative selection categories, respectively; the values of K_a/K_s are divided arbitrarily into four categories, $K_a/K_s > 1.05$, $1.05 > K_a/K_s > 0.95$, $0.95 > K_a/K_s > 0.5$, and $0.5 > K_a/K_s$, which correspond to their selection categories, respectively. Fixation probability has been calculated in the approximation of $\Delta\Delta\psi_{ND} \simeq \Delta\psi_N$; see Eqs. 8 and 22. The distribution of $\Delta\psi_N$ due to single nucleotide nonsynonymous mutations is approximated by a log-normal distribution with $n_{\rm shift} = 2.0$; see Eqs. 27 and 31. The standard deviation of $\Delta\psi_N$ is determined to satisfy $\langle\Delta\psi_N\rangle_{\rm fixed} = 0$ at $\overline{\Delta\psi_N}(= \overline{\Delta\psi_N^{\rm eq}})$.

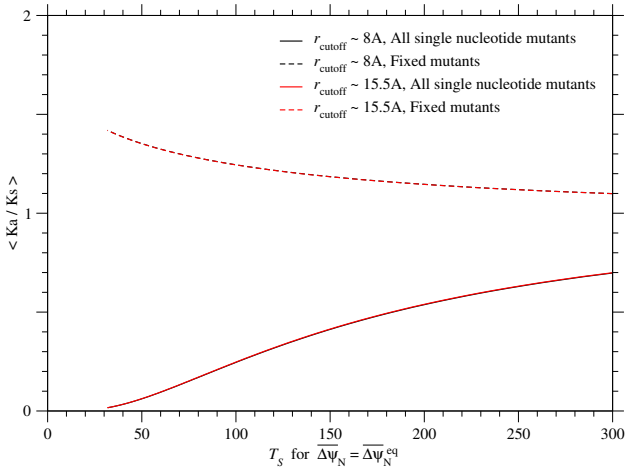

Figure 9: **The averages of K_a/Ks over all single nucleotide nonsynonymous mutations and over their fixed mutations as a function of the effective temperature of selection, T_s, at equilibrium, $\langle\Delta\psi_N\rangle_{\mathbf{fixed}} = 0$.** Solid and broken lines indicate $\langle K_a/K_s\rangle$ and $\langle K_a/K_s\rangle_{\rm fixed}$, respectively. Fixation probability has been calculated in the approximation of $\Delta\Delta\psi_{ND} \simeq \Delta\psi_N$; see Eqs. 8 and 22. The distribution of $\Delta\psi_N$ due to single nucleotide nonsynonymous mutations is approximated by a log-normal distribution with $n_{\rm shift} = 2.0$; see Eqs. 27 and 31. The standard deviation of $\Delta\psi_N$ is determined to satisfy $\langle\Delta\psi_N\rangle_{\rm fixed} = 0$ at $\overline{\Delta\psi_N}(= \overline{\Delta\psi}_N^{\rm eq})$. The T_s is estimated in the scale relative to the T_s of the PDZ family in the approximation (11) that the variance of ΔG_N due to single nucleotide nonsynonymous mutations is constant irrespective of protein families; see Eq. 5. The curves for $r_{\rm cutoff} \sim 8$ and 15.5Å almost overlap with each other.

Supplementary material
for
"Selection originating from protein foldability:
II. Folding free energy, sequence emsemble, and fitness"

Sanzo Miyazawa
sanzo.miyazawa@gmail.com

1 Methods

1.1 Knowledge of protein folding

A protein folding theory (3), which is based on a random energy model (REM), indicates that the equilibrium ensemble of amino acid sequences, $\boldsymbol{\sigma} = (\sigma_1, \cdots, \sigma_L)$ where σ_i is the type of amino acid at site i and L is sequence length, should be a canonical ensemble with a Boltzmann factor consisting of the folding free energy, $\Delta G_{ND}(\boldsymbol{\sigma}, T)$ and an effective temperature T_s of natural selection.

$$P(\boldsymbol{\sigma}) \propto P^{\rm mut}(\boldsymbol{\sigma}) \exp(\frac{-\Delta G_{ND}(\boldsymbol{\sigma}, T)}{k_B T_s}) \tag{S1}$$

$$\propto \exp(\frac{-G_N(\boldsymbol{\sigma})}{k_B T_s}) \qquad \text{if } \boldsymbol{f}(\boldsymbol{\sigma}) = \text{constant} \tag{S2}$$

$$\Delta G_{ND}(\boldsymbol{\sigma}, T) \equiv G_N(\boldsymbol{\sigma}) - G_D(\boldsymbol{f}(\boldsymbol{\sigma}), T) \tag{S3}$$

where $p^{\rm mut}(\boldsymbol{f}(\boldsymbol{\sigma}))$ is the probability of a sequence ($\boldsymbol{\sigma}$) randomly occurring in a mutational process and depends only on the amino acid frequencies $\boldsymbol{f}(\boldsymbol{\sigma})$, k_B is the Boltzmann constant, T is a growth temperature, and G_N and G_D are the free energies of the native conformation and denatured state, respectively. Selection temperature T_s quantifies how strong the folding constraints have been during evolution (20), and is specific to the protein structure and function. The free energy G_D of the denatured state does not depend on the amino acid order but the amino acid composition, $\boldsymbol{f}(\boldsymbol{\sigma})$, in a sequence. It is reasonable to assume that mutations independently occur between sites, and therefore the equilibrium frequency of a sequence in the mutational process is equal to the product of the equilibrium frequencies over sites; $P^{\rm mut}(\boldsymbol{\sigma}) = \prod_i p^{\rm mut}(\sigma_i)$, where $p^{\rm mut}(\sigma_i)$ is the equilibrium frequency of σ_i at site i in the mutational process.

The distribution of conformational energies in the denatured state (molten globule state), which consists of conformations as compact as the native conformation. is approximated in the random energy model (REM), particularly the independent interaction model (IIM) (3), to be equal to the energy distribution of randomized sequences, which is then approximated by a Gaussian distribution, in the native conformation. That is, a partition function Z for the denatured state is written as follows with the energy density $n(E)$ of conformations that is approximated by a product of a Gaussian probability density and the total number of conformations whose logarithm is proportional to the chain length.

$$Z = \int \exp(\frac{-E}{k_B T})\, n(E) dE \tag{S4}$$

$$n(E) \approx \exp(\omega L) \mathcal{N}(\bar{E}(\boldsymbol{f}(\boldsymbol{\sigma})), \delta E^2(\boldsymbol{f}(\boldsymbol{\sigma}))) \tag{S5}$$

where ω is the conformational entropy per residue in the compact denatured state, and $\mathcal{N}(\bar{E}(\boldsymbol{f}(\boldsymbol{\sigma})), \delta E^2(\boldsymbol{f}(\boldsymbol{\sigma})))$ is the Gaussian probability density with mean $\bar{E}$ and variance δE^2, which depend only on the amino acid composition of the protein sequence. The free energy of the denatured state is approximated as follows.

$$G_D(\boldsymbol{f}(\boldsymbol{\sigma}), T) \approx \bar{E}(\boldsymbol{f}(\boldsymbol{\sigma})) - \frac{\delta E^2(\boldsymbol{f}(\boldsymbol{\sigma}))}{2k_B T} - k_B T \omega L \tag{S6}$$

$$= \bar{E}(\boldsymbol{f}(\boldsymbol{\sigma})) - \delta E^2(\boldsymbol{f}(\boldsymbol{\sigma})) \frac{\vartheta(T/T_g)}{k_B T} \tag{S7}$$

$$\vartheta(T/T_g) \equiv \begin{cases} \frac{1}{2}(1 + \frac{T^2}{T_g^2}) & \text{for } T > T_g \\ \frac{T}{T_g} & \text{for } T \le T_g \end{cases} \tag{S8}$$

where $\bar{E}$ and δE^2 are estimated as the mean and variance of interaction energies of randomized sequences in the native conformation. T_g is the glass transition temperature of the protein at which entropy becomes zero (3).

$$-\frac{\partial G_D}{\partial T}|_{T=T_g} = 0 \tag{S9}$$

The conformational entropy per residue ω in the compact denatured state can be represented with T_g.

$$\omega L = \frac{\delta E^2}{2(k_B T_g)^2} \tag{S10}$$

Thus, unless $T_g < T_m$, a protein will be trapped at local minima on a rugged free energy landscape before it can fold into a unique native structure.

1.2 Probability distribution of homologous sequences in sequence space

The probability distribution $P(\boldsymbol{\sigma})$ of sequences, $\boldsymbol{\sigma} = (\sigma_1, \cdots, \sigma_L)$ where $\sigma_i \in \{\text{amino acids, deletion}\}$, in sequence space with maximum entropy, which satisfies a given amino acid frequency at each site and a given pairwise amino acid frequency at each site pair, is a Boltzmann distribution (4, 5).

$$P(\boldsymbol{\sigma}) \propto \exp(-\psi_N(\boldsymbol{\sigma})) \tag{S11}$$

$$\psi_N(\boldsymbol{\sigma}) \equiv -(\sum_i^L (h_i(\sigma_i) + \sum_{j>i} J_{ij}(\sigma_i, \sigma_j))) \tag{S12}$$

where h_i and J_{ij} are one-body and two-body interactions and must satisfy the following constraints.

$$\sum_{\boldsymbol{\sigma}, \sigma_i = a_k} P(\boldsymbol{\sigma}) = P_i(a_k) \tag{S13}$$

$$\sum_{\boldsymbol{\sigma}, \sigma_i = a_k, \sigma_j = a_l} P(\boldsymbol{\sigma}) = P_{ij}(a_k, a_l) \tag{S14}$$

where $P_i(a_k)$ is the frequency of amino acid a_k at site i and $P_{ij}(a_k, a_l)$ is the frequency of amino acid pair, a_k at i and a_l at j; $a_k \in \{\text{amino acids, deletion}\}$. The pairwise interaction matrix J satisfies $J_{ij}(a_k, a_l) = J_{ji}(a_l, a_k)$ and $J_{ii}(a_k, a_l) = 0$. Interactions h_i and J_{ij} can be well estimated from a multiple sequence alignment (MSA) in the mean field approximation (4, 5), or by maximizing a pseudo-likelihood (6, 7). Here we must notice that $\psi_N(\boldsymbol{\sigma})$ has been estimated under the constraints on amino acid compositions at all sites, and therefore the amino acid composition of a whole sequence must be constant across sequences.

From Eqs. S2 and S11,

$$G_N(\boldsymbol{\sigma}) = k_B T_s[\,\psi_N(\boldsymbol{\sigma}) + \text{function of} \boldsymbol{f}(\boldsymbol{\sigma})\,] \tag{S15}$$

$$G_D(\boldsymbol{f}(\boldsymbol{\sigma}), T) = k_B T_s[\,\psi_D(\boldsymbol{\sigma}) + \text{function of} \boldsymbol{f}(\boldsymbol{\sigma})\,] \tag{S16}$$

$$\Delta G_{ND}(\boldsymbol{\sigma}, T) = k_B T_s\, \Delta\psi_{ND}(\boldsymbol{\sigma}) \tag{S17}$$

$$\Delta\psi_{ND}(\boldsymbol{\sigma}) \equiv \psi_N(\boldsymbol{\sigma}) - \psi_D(\boldsymbol{\sigma}) \tag{S18}$$

$$\psi_D(\boldsymbol{\sigma}) \approx \bar{\psi}(\boldsymbol{f}(\boldsymbol{\sigma})) - \delta\psi^2(\boldsymbol{f}(\boldsymbol{\sigma}))\vartheta(T/T_g)T_s/T \tag{S19}$$

$$\omega = (T_s/T_g)^2\delta\psi^2/(2L) \tag{S20}$$

where $\bar{E} = k_B T_s \bar{\psi}$ and $\delta E^2 = (k_B T_s)^2 \delta\psi^2$. The mean $\bar{\psi}$ and variance $\Delta\psi^2$ are estimated as the mean and variance of ψ_N over randomized sequences in the native structure (3).

1.3 The equilibrium distribution of sequences in a mutation-fixation process

Here we assume that the mutational process is a reversible Markov process. That is, the mutation rate per gene, $M_{\boldsymbol{\mu\nu}}$, from sequence $\boldsymbol{\mu} \equiv (\mu_1, \cdots, \mu_L)$ to $\boldsymbol{\nu}$ satisfies the detailed balance condition

$$P^{\text{mut}}(\boldsymbol{\mu}) M_{\mu\nu} = P^{\text{mut}}(\boldsymbol{\nu}) M_{\boldsymbol{\nu\mu}} \tag{S21}$$

where $P^{\rm mut}(\boldsymbol{\nu})$ is the equilibrium frequency of sequence $\boldsymbol{\nu}$ in a mutational process, $M_{\mu\nu}$. The mutation rate per population is equal to $2NM_{\mu\nu}$ for a duploid population, where N is the population size. The substitution rate is equal to the product of the mutation rate and the fixation rate.

$$R_{\mu\nu} = 2NM_{\mu\nu}u(s(\boldsymbol{\mu} \to \boldsymbol{\nu})) \tag{S22}$$

where $u(s(\boldsymbol{\mu} \to \boldsymbol{\nu}))$ is the fixation probability of mutants from $\boldsymbol{\mu}$ to $\boldsymbol{\nu}$ the selective advantage of which is equal to s.

In a duploid population, the fixation probability, u, of a mutant, the selective advantage of which is equal to s and the frequency of which in a population is equal to q_m, was estimated (18) as

$$2Nu(s) = 2N\frac{1-e^{-4N_e s q_m}}{1-e^{-4N_e s}} \tag{S23}$$

$$= \frac{u(s)}{u(0)} \qquad \text{with} \qquad q_{\rm m} = \frac{1}{2N} \qquad \text{for duploid} \tag{S24}$$

where N_e is an effective population size. The selective advantage of a mutant sequence $\boldsymbol{\nu}$ to a wildtype $\boldsymbol{\mu}$ is equal to

$$s(\boldsymbol{\mu} \to \boldsymbol{\nu}) = m(\boldsymbol{\nu}) - m(\boldsymbol{\mu}) \tag{S25}$$

where $m(\boldsymbol{\nu})$ is the Malthusian fitness of a mutant sequence, and $m(\boldsymbol{\mu})$ is for the wildtype.

This Markov process of substitutions in sequence is reversible, and the equilibrium frequency, $P^{\rm eq}(\boldsymbol{\mu})$, for each sequence is represented by

$$P^{\rm eq}(\boldsymbol{\mu}) = \frac{P^{\rm mut}(\boldsymbol{\mu})\exp(4N_e m(\boldsymbol{\mu})(1-q_m))}{\sum_{\nu} P^{\rm mut}(\boldsymbol{\nu})\exp(4N_e m(\boldsymbol{\nu})(1-q_m))} \tag{S26}$$

because both the mutation and fixation processes satisfy the detailed balance conditions, Eq. S21 and the following equation, respectively.

$$\exp(4N_e m(\boldsymbol{\mu})(1-q_m))u(s(\boldsymbol{\mu} \to \boldsymbol{\nu}))$$

$$= \frac{\exp(-4N_e m(\boldsymbol{\mu})q_m) - \exp(-4N_e m(\boldsymbol{\nu})q_m)}{\exp(-4N_e m(\boldsymbol{\mu})) - \exp(-4N_e m(\boldsymbol{\nu}))} \tag{S27}$$

$$= \exp(4N_e m(\boldsymbol{\nu})(1-q_m))u(s(\boldsymbol{\nu} \to \boldsymbol{\mu})) \tag{S28}$$

As a result, the ensemble of homologous sequences in molecular evolution obeys a Boltzmann distribution.

1.4 Relationships between $m(\boldsymbol{\sigma})$, $\psi_N(\boldsymbol{\sigma})$, and $\Delta G_{ND}(\boldsymbol{\sigma})$ of protein sequence

From Eqs. S1, S17, S18, and S26 , we can get the following relationships among the Malthusian fitness m, the folding free energy change ΔG_{ND} and $\Delta\psi_{ND}$ of protein sequence.

$$P^{\rm eq}(\boldsymbol{\mu}) = \frac{P^{\rm mut}(\boldsymbol{\mu})\exp(4N_e m(\boldsymbol{\mu})(1-q_m))}{\sum_{\nu} P^{\rm mut}(\boldsymbol{\nu})\exp(4N_e m(\boldsymbol{\nu})(1-q_m)))} \tag{S29}$$

$$= \frac{P^{\rm mut}(\boldsymbol{\mu})\exp(-\Delta G_{ND}(\boldsymbol{\mu},T)/(k_B T_s))}{\sum_{\nu} P^{\rm mut}(\boldsymbol{\nu})\exp(-\Delta G_{ND}(\boldsymbol{\nu},T)/(k_B T_s))} \tag{S30}$$

$$= \frac{P^{\rm mut}(\boldsymbol{\mu})\exp(-\Delta\psi_{ND}(\boldsymbol{\mu}))}{\sum_{\nu} P^{\rm mut}(\boldsymbol{\mu})\exp(-\Delta\psi_{ND}(\boldsymbol{\nu}))} \tag{S31}$$

Then, the following relationships are derived.

$$4N_e m(\boldsymbol{\mu})(1-q_m)$$

$$= \frac{-\Delta G_{ND}(\boldsymbol{\mu},T)}{k_B T_s} + \text{constant} \tag{S32}$$

$$= -\Delta\psi_{ND}(\boldsymbol{\mu},T) + \text{constant} \tag{S33}$$

$$= -[\,\psi_N(\boldsymbol{\mu}) - \bar{\psi}(\boldsymbol{f}(\boldsymbol{\mu})) + \delta\psi^2(\boldsymbol{f}(\boldsymbol{\mu}))\vartheta(T/T_g)T_s/T\,] + \text{constant} \tag{S34}$$

Selective advantage is

$$
\begin{aligned}
4N_e s(\boldsymbol{\mu} \to \boldsymbol{\nu})(1-q_m) &= (4N_e m(\boldsymbol{\nu}) - 4N_e m(\boldsymbol{\mu}))(1-q_m) && \text{(S35)}\\
&= -(\Delta G_{ND}(\boldsymbol{\nu},T) - \Delta G_{ND}(\boldsymbol{\mu},T))/(k_B T_s) && \text{(S36)}\\
&= -(\Delta\psi_{ND}(\boldsymbol{\nu},T) - \Delta\psi_{ND}(\boldsymbol{\mu},T)) && \text{(S37)}\\
&= -(G_N(\boldsymbol{\nu}) - G_N(\boldsymbol{\mu}))/(k_B T_s) = -(\psi_N(\boldsymbol{\nu}) - \psi_N(\boldsymbol{\mu})) \qquad \text{if } \boldsymbol{f}(\boldsymbol{\mu}) = \boldsymbol{f}(\boldsymbol{\nu}) && \text{(S38)}
\end{aligned}
$$

1.5 The ensemble average of folding free energy, $\Delta G_{ND}(\boldsymbol{\sigma},T)$, over sequences

The ensemble average of $\Delta G_{ND}(\boldsymbol{\sigma},T)$ over sequences with Eq. S1 is

$$
\begin{aligned}
&\langle \Delta G_{ND}(\boldsymbol{\sigma},T)\rangle_{\boldsymbol{\sigma}} && \text{(S39)}\\
&\equiv \frac{1}{Z_\sigma}\sum_{\boldsymbol{\sigma}} \Delta G_{ND}(\boldsymbol{\sigma},T) P^{\mathrm{mut}}(\boldsymbol{\sigma}) \exp(-\frac{\Delta G_{ND}(\boldsymbol{\sigma},T)}{k_B T_s}) && \text{(S40)}\\
&\approx \frac{1}{Z_\sigma}\Big[\sum_{\boldsymbol{\sigma}\,|\,\boldsymbol{f}(\boldsymbol{\sigma})=\overline{\boldsymbol{f}(\boldsymbol{\sigma}_N)}} G_N(\boldsymbol{\sigma}) \exp(-\frac{G_N(\boldsymbol{\sigma})}{k_B T_s}) \Big] - G_D(\overline{\boldsymbol{f}(\boldsymbol{\sigma}_N)},T) && \text{(S41)}\\
&= \langle G_N(\boldsymbol{\sigma})\rangle_{\boldsymbol{\sigma}} - G_D(\overline{\boldsymbol{f}(\boldsymbol{\sigma}_N)},T) && \text{(S42)}
\end{aligned}
$$

where $\boldsymbol{\sigma}_N$ denotes a native sequence, and $\overline{\boldsymbol{f}(\boldsymbol{\sigma}_N)}$ denotes the average of $\boldsymbol{f}(\boldsymbol{\sigma}_N)$ over homologous sequences. In Eq. S41, the sum over all sequences is approximated by the sum over sequences the amino acid composition of which is the same as that of the native sequences. The ensemble average of G_N is also estimated in the Gaussian approximation (3).

$$
\begin{aligned}
\langle G_N(\boldsymbol{\sigma})\rangle_{\boldsymbol{\sigma}} &\approx \frac{\int E\exp(-E/(k_B T_s))\, n(E)\, dE}{\int \exp(-E/(k_B T_s))\, n(E)\, dE} && \text{(S43)}\\
&= \bar{E}(\overline{\boldsymbol{f}(\boldsymbol{\sigma}_N)}) - \delta E^2(\overline{\boldsymbol{f}(\boldsymbol{\sigma}_N)})/(k_B T_s) && \text{(S44)}\\
\langle \psi_N(\boldsymbol{\sigma})\rangle_{\boldsymbol{\sigma}} &\approx \bar{\psi}(\overline{\boldsymbol{f}(\boldsymbol{\sigma}_N)}) - \delta\psi^2(\overline{\boldsymbol{f}(\boldsymbol{\sigma}_N)}) && \text{(S45)}
\end{aligned}
$$

The ensemble averages of $\Delta G_{ND}(\boldsymbol{\sigma},T)$ and $\psi_N(\boldsymbol{\sigma})$ over sequences are observable as the sample averages of $\Delta G_{ND}(\boldsymbol{\sigma}_N,T)$ and $\psi_N(\boldsymbol{\sigma}_N)$ over homologous sequences fixed in protein evolution, respectively.

$$
\begin{aligned}
\overline{\Delta G_{ND}(\boldsymbol{\sigma}_N,T)} &= \langle \Delta G_{ND}(\boldsymbol{\sigma},T)\rangle_{\boldsymbol{\sigma}} && \text{(S46)}\\
&\approx \delta E^2(\overline{\boldsymbol{f}(\boldsymbol{\sigma}_N)})\,[\,\vartheta(T/T_g)T_s/T - 1\,] && \text{(S47)}\\
&= k_B T_s \delta\psi^2(\overline{\boldsymbol{f}(\boldsymbol{\sigma}_N)})\,[\,\vartheta(T/T_g)T_s/T - 1\,] && \text{(S48)}\\
\overline{\psi_N(\boldsymbol{\sigma}_N)} &\equiv \frac{\sum_{\boldsymbol{\sigma}_N} w_{\boldsymbol{\sigma}_N}\psi_N(\boldsymbol{\sigma}_N)}{\sum_{\boldsymbol{\sigma}_N} w_{\boldsymbol{\sigma}_N}} && \text{(S49)}\\
&= \langle \psi_N(\boldsymbol{\sigma})\rangle_{\boldsymbol{\sigma}} && \text{(S50)}
\end{aligned}
$$

where the overline denotes sample average with a sample weight $w_{\boldsymbol{\sigma}_N}$ for each homologous sequence, which is used to reduce phylogenetic biases in the set of homologous sequences.

The folding free energy becomes equal to zero at the melting temperature T_m; $\langle \Delta G_{ND}(\boldsymbol{\sigma}_N,T_m)\rangle_{\boldsymbol{\sigma}} = 0$. Thus, the following relationship must be satisfied (3).

$$
\vartheta(T_m/T_g)\frac{T_s}{T_m} = \frac{T_s}{2T_m}(1+\frac{T_m^2}{T_g^2}) = 1 \quad \text{with } T_s \le T_g \le T_m \qquad \text{(S51)}
$$

1.6 Estimation of $\bar{\psi}(\boldsymbol{f}(\boldsymbol{\sigma}))$ and $\delta\psi^2(\boldsymbol{f}(\boldsymbol{\sigma}))$

The mean $\bar{\psi}(\boldsymbol{f}(\boldsymbol{\sigma}))$ and the variance $\delta\psi^2(\boldsymbol{f}(\boldsymbol{\sigma}))$ in the Gaussian approximation for the distribution of conformational energies at the denatured state are estimated as the mean and variance of ψ_N of random sequences in the native conformation (3).

$$
\bar{\psi}(\boldsymbol{f}(\boldsymbol{\sigma})) = -\sum_i [h_i(::) + \sum_{j>i} J_{ij}(::,::)] \qquad \text{(S52)}
$$

where $h_i(::)$ and $J_{ij}(::,::)$ are the means of one-body and two-body interactions in random sequences.

$$h_i(::) \equiv \sum_k h_i(a_k) f_{a_k}(\boldsymbol{\sigma}) \tag{S53}$$

$$J_{ij}(::,::) \equiv \sum_k \sum_l J_{ij}(a_k, a_l) f_{a_k}(\boldsymbol{\sigma}) f_{a_l}(\boldsymbol{\sigma}) \tag{S54}$$

where $f_{a_k}(\boldsymbol{\sigma})$ is the composition of amino acid a_k in the sequence $\boldsymbol{\sigma}$.

$$f_{a_k}(\boldsymbol{\sigma}) = \frac{1}{L} \sum_{i=1}^{L} \delta_{\sigma_i a_k} \tag{S55}$$

where $\delta_{\sigma_i a_k}$ is the Kronecker delta. The variance, $\delta\psi^2(\boldsymbol{f}(\boldsymbol{\sigma}))$, is

$$\delta\psi^2(\boldsymbol{f}(\boldsymbol{\sigma})) = \sum_k f_{a_k}(\boldsymbol{\sigma}) \sum_i [\, \delta h_i(a_k)^2 + \sum_{j \neq i} \{\, 2\delta h_i(a_k) \delta J_{ij}(a_k, ::) \tag{S56}$$

$$+ \sum_{m \neq \{i,j\}} \delta J_{ij}(a_k, ::) \delta J_{im}(a_k, ::) + \frac{1}{2} \sum_l \delta J_{ij}(a_k, a_l)^2 f_{a_l}(\boldsymbol{\sigma}) \,\} \,] \tag{S57}$$

where

$$\delta h_i(a_k) \equiv h_i(a_k) - h_i(::) \tag{S58}$$

$$\delta J_{ij}(a_k, ::) \equiv J_{ij}(a_k, ::) - J_{ij}(::,::) \tag{S59}$$

$$\delta J_{ij}(a_k, a_l) \equiv J_{ij}(a_k, a_l) - J_{ij}(::,::) \tag{S60}$$

1.7 Estimation of one-body (h) and pairwise (J) interactions

The estimates of h and J (4, 5) are noisy, and J_{ij} may take significant values even for site pairs that are distantly located in the three dimensional structure of protein. Therefore, according to Morcos et al. (20), the estimate of J is modified as follows.

$$\hat{J}_{ij}(a_k, a_l) = J^{\mathrm{g}}_{ij}(a_k, a_l) H(r_{\mathrm{cutoff}} - r_{ij}) \tag{S61}$$

where J^{g} is the statistical estimate of J in a certain gauge, H is the Heaviside step function, and r_{ij} is the distance between the centers of amino acid side chains in protein structure, and r_{cutoff} is a distance threshold for residue pairwise interactions. Maximum interaction ranges employed for pairwise interactions are $r_{\mathrm{cutoff}} \sim 8$ and 15.5Å , which correspond to the first and second interaction shells between residues, respectively. Here it should be noticed that the total interaction $\psi_N(\boldsymbol{\sigma})$ defined by Eq. S12 does not depend on any gauge unless the interaction range for pairwise interactions is limited, but a gauge conversion in which interconversions between h and J occur may change the estimate of $\psi_N(\boldsymbol{\sigma})$ in the present scheme of Eq. S61 in which pairwise interactions are cut off at a certain distance. Thus, a natural gauge must be used before calculating $\hat{J}$.

For example, let us think about the Ising gauge (7), in which h^I and J^I can be calculated from any gauge through the following conversions.

$$J^{\mathrm{I}}_{ij}(a_k, a_l) = J^{\mathrm{g}}_{ij}(a_k, a_l) - J^{\mathrm{g}}_{ij}(a_k, :) - J^{\mathrm{g}}_{ij}(:, a_l) + J^{\mathrm{g}}_{ij}(:,:) \tag{S62}$$

$$h^{\mathrm{I}}(a_k) = h^{\mathrm{g}}_i(a_k) - h^{\mathrm{g}}_i(:) + \sum_{j \neq i} (J^{\mathrm{g}}_{ij}(a_k, :) - J^{\mathrm{g}}_{ij}(:,:)) \tag{S63}$$

where

$$h_i(:) \equiv \frac{1}{q} \sum_{k=1}^{q} h_i(a_k) \tag{S64}$$

$$J_{ij}(:,:) \equiv \frac{1}{q^2} \sum_{k=1}^{q} \sum_{l=1}^{q} J_{ij}(a_k, a_l) \tag{S65}$$

where q is equal to the total number of amino acid types including deletion, that is, $q = 21$. Thus, the gauge conversion of $\hat{J}$ does not affect the total interaction $\psi_N(\boldsymbol{\sigma})$ but the gauge conversion before calculating $\hat{J}$ may significantly change the total interaction.

In the DCA (4, 5), the interaction terms are estimated in the mean field approximation as follows.

$$J^{\mathrm{q}}_{ij}(a_k, a_l) = -(C^{-1})_{ij}(a_k, a_l) \tag{S66}$$

$$J^{\mathrm{q}}_{ij}(a_q, a_l) = J^{\mathrm{q}}_{ij}(a_k, a_q) = J^{\mathrm{q}}_{ij}(a_q, a_q) = 0 \tag{S67}$$

where $i \neq j$ and $1 \leq k, l \leq q-1$, and the covariance matrix C is defined as

$$C_{ij}(a_k, a_l) \equiv P_{ij}(a_k, a_l) - P_i(a_k)P_j(a_l) \tag{S68}$$

Here, one (a_q) of the amino acid types including deletion is used as the reference state; J^{q} denotes the J in this gauge. According to Morcos et al. (4), the probability $P_i(a_k)$ of amino acid a_k at site i and the joint probabilities $P_{ij}(a_k, a_l)$ of amino acids, a_k at site i and a_l at site j, are evaluated by

$$P_i(a_k) = (1 - p_c)f_i(a_k) + p_c\frac{1}{q} \tag{S69}$$

$$P_{ij}(a_k, a_l) = (1 - p_c)f_{ij}(a_k, a_l) + p_c\frac{1}{q^2} \qquad \text{for} \quad i \neq j \tag{S70}$$

$$P_{ii}(a_k, a_l) = P_i(a_k)\delta_{a_k a_l} \tag{S71}$$

where $0 \leq p_c \leq 1$ is the ratio of pseudocount, and $f_i(a_k)$ is the frequency of amino acid a_k at site i and $f_{ij}(a_k, a_l)$ is the frequency of the site pair, a_k at i and a_l at j, in an alignment; $f_{ii}(a_k, a_l)$ is defined as $f_{ii}(a_k, a_l) = f_i(a_k)\delta_{a_k a_l}$. Then, according to Morcos et al. (4), the one body interactions $h_i(a_k)$ are estimated in the isolated two-state model, that is,

$$P_i(a_k) \propto \exp\left[\, h^{\mathrm{q}}_{ij}(a_k) + J^{\mathrm{q}}_{ij}(a_k, a_l) + h^{\mathrm{q}}_{ji}(a_l) \,\right] \tag{S72}$$

$$h^{\mathrm{q}}_i(a_k) = \frac{1}{L-1}\sum_{j \neq i} h^{\mathrm{q}}_{ij}(a_k) \tag{S73}$$

These h^q and J^q in the q gauge are converted to a new gauge, which is called a simple gauge here,

$$h^{\mathrm{s}}_i(a_k) = h^{\mathrm{q}}_i(a_k) - h^{\mathrm{q}}_i(:) \tag{S74}$$

$$J^{\mathrm{s}}_{ij}(a_k, a_l) = J^{\mathrm{q}}_{ij}(a_k, a_l) - J^{\mathrm{q}}_{ij}(:, :) \tag{S75}$$

In this gauge, the reference state is the average state over amino acids including deletion, instead of a specific amino acid (a_q) in the q gauge. The estimate of J in this gauge is used to calculate $\hat{J}$ in Eq. S61.

Distribution of $\Delta\Delta\psi_{ND} \simeq \Delta\psi_N$ due to single nucleotide nonsynonymous substitutions

The probability density function (PDF) of $\Delta\Delta\psi_{ND}$, $p(\Delta\Delta\psi_{ND})$, due to single nucleotide nonsynonymous substitutions is approximated by the PDF of $\Delta\psi_N$, $p(\Delta\psi_N)$, because $\Delta\psi_D \simeq 0$ for single amino acid substitutions.

$$\begin{aligned} \Delta\Delta\psi_{ND} &\simeq \Delta\psi_N & \text{(S76)} \\ p(\Delta\Delta\psi_{ND}) &\simeq p(\Delta\psi_N) & \text{(S77)} \end{aligned}$$

for single nucleotide nonsynonymous substitutions.

For simplicity, a log-normal distribution, $\ln \mathcal{N}(x;\mu,\sigma)$, for which x, μ and σ are defined as follows, is arbitrarily employed here to reproduce observed PDFs of $\Delta\psi_N$, particularly in the domain of $\Delta\psi_N < \overline{\Delta\psi_N}$, although other distributions such as inverse Γ distributions can equally reproduce the observed ones, too.

$$\begin{aligned} p(\Delta\psi_N) &\approx \ln \mathcal{N}(x;\mu,\sigma) \equiv \frac{1}{x}\mathcal{N}(\ln x;\mu,\sigma) & \text{(S78)} \\ x &\equiv \max(\Delta\psi_N - \Delta\psi_N^{\mathrm{o}}, 0) & \text{(S79)} \\ \exp(\mu + \sigma^2/2) &= \overline{\Delta\psi_N} - \Delta\psi_N^{\mathrm{o}} & \text{(S80)} \\ \exp(2\mu + \sigma^2)(\exp(\sigma^2) - 1) &= \overline{(\Delta\psi_N - \overline{\Delta\psi_N})^2}) & \text{(S81)} \\ \Delta\psi_N^{\mathrm{o}} &\equiv \min(\overline{\Delta\psi_N} - n_{\mathrm{shift}}\overline{(\Delta\psi_N - \overline{\Delta\psi_N})^2})^{1/2}, 0) & \text{(S82)} \end{aligned}$$

where $\Delta\psi_N^{\mathrm{o}}$ is the origin for the log-normal distribution and the shifting factor n_{shift} is taken to be equal to 2, unless specified.

Probability distributions of selective advantage, fixation rate and K_a/K_s

Now, we can consider the probability distributions of characteristic quantities that describe the evolution of genes. First of all, the PDF of selective advantage s, $p(s)$, of mutant genes can be represented by

$$\begin{aligned} p(s) &= p(\Delta\Delta\psi_{ND})\left|\frac{d\Delta\Delta\psi_{ND}}{ds}\right| \\ &= p(\Delta\Delta\psi_{ND})4N_e(1 - q_m) & \text{(S83)} \end{aligned}$$

where $\Delta\Delta\psi_N$ must be regarded as a function of s, that is, $\Delta\Delta\psi_N = -4N_e s(1 - q_m)$; see Eq. S38. The PDF of $4N_e s$, $p(4N_e s) = p(s)/(4Ne)$, may be more useful than $p(s)$.

The PDF of fixation probability u can be represented by

$$\begin{aligned} p(u) &= p(4N_e s)\frac{d4N_e s}{du} \\ &= p(4N_e s)\frac{(e^{4N_e s} - 1)^2 e^{4N_e s(q_m - 1)}}{q_m(e^{4N_e s} - 1) - (e^{4N_e s q_m} - 1)} & \text{(S84)} \end{aligned}$$

where s must be regarded as a function of u.

The ratio of the substitution rate per nonsynonymous site (K_a) for nonsynonymous substitutions with selective advantage s to the substitution rate per synonymous site (K_s) for synonymous substitutions with s = 0 is

$$\frac{K_a}{K_s} = \frac{u(s)}{u(0)} = \frac{u(s)}{q_m} \quad \text{(S85)}$$

assuming that synonymous substitutions are completely neutral and mutation rates at both types of sites are the same. The PDF of K_a/K_s is

$$p(K_a/K_s) = p(u)\frac{du}{d(K_a/K_s)} = p(u)\, q_m \quad \text{(S86)}$$

Probability distributions of $\Delta\Delta\psi_{ND}$, $4N_e s$, u, and K_a/K_s in fixed mutant genes

Now, let us consider fixed mutant genes. The PDF of $\Delta\Delta\psi_{ND}$ in fixed mutants is

$$p(\Delta\Delta\psi_{ND,\text{fixed}}) = p(\Delta\Delta\psi_{ND})\frac{u(s(\Delta\Delta\psi_{ND}))}{\langle u(s(\Delta\Delta\psi_{ND}))\rangle} \tag{S87}$$

$$\langle u\rangle \equiv \int_{-\infty}^{\infty} u(s)p(\Delta\Delta\psi_{ND})d\Delta\Delta\psi_{ND} \tag{S88}$$

Likewise, the PDF of selective advantage in fixed mutants is

$$p(4N_e s_{\text{fixed}}) = p(4N_e s)\frac{u(s)}{\langle u(s)\rangle} \tag{S89}$$

and those of the u and K_a/K_s in fixed mutants are

$$p(u_{\text{fixed}}) = p(u)\frac{u}{\langle u\rangle} \tag{S90}$$

$$p((\frac{K_a}{K_s})_{\text{fixed}}) = p(\frac{K_a}{K_s})\frac{u}{\langle u\rangle} = p(\frac{K_a}{K_s})\frac{\frac{K_a}{K_s}}{\langle\frac{K_a}{K_s}\rangle} \tag{S91}$$

The average of K_a/K_s in fixed mutants is equal to the ratio of the second moment to the first moment of K_a/K_s in all arising mutants.

$$\langle\frac{K_a}{K_s}\rangle_{\text{fixed}} = \langle(\frac{K_a}{K_s})^2\rangle/\langle\frac{K_a}{K_s}\rangle \tag{S92}$$

2 Materials

2.1 Sequence data

We study the single domains of 8 Pfam (19) families and both the single domains and multi-domains from 3 Pfam families. In Table S1, their Pfam ID for a multiple sequence alignment, and Uniprot ID and PDB ID with the starting- and ending-residue positions of the domains are listed. The full alignments for their families at the Pfam are used to estimate one-body interactions h and pairwise interactions J with the DCA program from "http://dca.rice.edu/portal/dca/home" (4, 5). To estimate the sample ($\overline{\psi_N}$) and ensemble ($\langle\psi_N\rangle_{\boldsymbol{\sigma}}$) averages of the total interaction, M unique sequences with no deletion are used. In order to reduce phylogenetic biases in the set of homologous sequences, we employ a sample weight ($w_{\boldsymbol{\sigma}_N}$) for each sequence, which is equal to the inverse of the number of sequences that are less than 20% different from a given sequence in a given set of homologous sequences. Only representatives of unique sequences with no deletion, which are at least 20% different from each other, are used to calculate the changes of the total interaction ($\Delta\psi_N$) due to single nucleotide nonsynonymous substitutions; the number of the representatives is almost equal to M_{eff} in Table S1.

3 Empirical rules found in the analysis of $\Delta\psi_N$

In the preceding manuscript (11), We examined the changes of ψ_N due to single nucleotide nonsynonymous substitutions over all sites in the homologous sequences of 14 protein families, and found the following regression equation.

$$\overline{\Delta\psi_N} \approx \alpha_{\psi_N}\frac{\psi_N - \overline{\psi_N}}{L} + \overline{\overline{\Delta\psi_N}} \qquad \text{with } \alpha_{\psi_N} < 0 \tag{S93}$$

with correlation coefficients, $r_{\psi_N} > 0.9$, where L is sequence length, $\overline{\psi_N}$ denotes the average of ψ_N over all homologous sequences, and $\overline{\Delta\psi_N}$ and $\overline{\overline{\Delta\psi_N}}$ denote the average of $\Delta\psi_N$ over all single nucleotide synonymous substitutions at all sites in a protein sequence and its total average over all homologous sequences in a protein family, respectively. In addition, the following relationship for the variance of $\Delta\psi_N$ was found.

$$\text{Var}(\Delta\psi_N) \approx \text{independent of } \psi_N \text{ and constant across homologous sequences in every protein family} \tag{S94}$$

$$= \text{function of } k_B T_s \tag{S95}$$

Because

$$\mathrm{Var}(\Delta G_N) \quad = \quad \text{function that must not explicitly depend on } k_B T_s \text{ but } G_N \tag{S96}$$

the following important relationship was derived and used to estimate the relative value of T_s against $T_{s,\mathrm{PDZ}}$ of the PDZ family.

$$\begin{aligned} \mathrm{Var}(\Delta G_N) &= (k_B T_s)^2 \mathrm{Var}(\Delta \psi_N) \\ &\approx \text{constant} \end{aligned} \tag{S97}$$

where $\mathrm{Var}(\Delta G_N)$ and $\mathrm{Var}(\Delta \psi_N)$ are the variances of ΔG_N and $\Delta \psi_N$ over all single nucleotide nonsynonymous substitutions at all sites, respectively. These relationships, Eqs. S93 and S97, are also shown in Figs. S3 and S4 , and the regression coefficients (α_{ψ_N}) and correlation coefficients (r_{ψ_N}) are listed in Tables S2 and S5. With estimated T_s and experimental melting temperature T_m, glass transition temperature T_g and folding free energy ΔG_N were estimated for each protein family on the basis of the REM. The estimates of T_s and T_g are all within a reasonable range, and the estimated values of ΔG_N agree well with their experimental values for 5 protein families, justifying the estimates of T_s.

Table S1: **Protein families, and structures studied.**

Pfam family	UniProt ID	N [a]	N_{eff} [bc]	M [d]	M_{eff} [ce]	L [f]	PDB ID
HTH_3	RPC1_BP434/7-59	15315(15917)	11691.21	6286	4893.73	53	1R69-A:6-58
Nitroreductase	Q97IT9_CLOAB/4-76	6008(6084)	4912.96	1057	854.71	73	3E10-A/B:4-76
SBP_bac_3 [g]	GLNH_ECOLI/27-244	9874(9972)	7374.96	140	99.70	218	1WDN-A:5-222
SBP_bac_3	GLNH_ECOLI/111-204	9712(9898)	7442.85	829	689.64	94	1WDN-A:89-182
OmpA	PAL_ECOLI/73-167	6035(6070)	4920.44	2207	1761.24	95	1OAP-A:52-146
DnaB	DNAB_ECOLI/31-128	1929(1957)	1284.94	1187	697.30	98	1JWE-A:30-127
LysR_substrate [g]	BENM_ACIAD/90-280	25138(25226)	20707.06	85(1)	67.00	191	2F6G-A/B:90-280
LysR_substrate	BENM_ACIAD/163-265	25032(25164)	21144.74	121(1)	99.27	103	2F6G-A/B:163-265
Methyltransf_5 [g]	RSMH_THEMA/8-292	1942(1953)	1286.67	578(2)	357.97	285	1N2X-A:8-292
Methyltransf_5	RSMH_THEMA/137-216	1877(1911)	1033.35	975(2)	465.53	80	1N2X-A:137-216
SH3_1	SRC_HUMAN:90-137	9716(16621)	3842.47	1191	458.31	48	1FMK-A:87-134
ACBP	ACBP_BOVIN/3-82	2130(2526)	1039.06	161	70.72	80	2ABD-A:2-81
PDZ	PTN13_MOUSE/1358-1438	13814(23726)	4748.76	1255	339.99	81	1GM1-A:16-96
Copper-bind	AZUR_PSEAE:24-148	1136(1169)	841.56	67(1)	45.23	125	5AZU-A/B/C/D:4-128

[a] The number of unique sequences and the total number of sequences in parentheses; the full alignments in the Pfam (19) are used.
[b] The effective number of sequences.
[c] A sample weight (w_{σ_N}) for a given sequence is equal to the inverse of the number of sequences that are less than 20% different from the given sequence.
[d] The number of unique sequences that include no deletion unless specified. The number in parentheses indicates the maximum number of deletions allowed.
[e] The effective number of unique sequences that include no deletion or at most the specified number of deletions.
[f] The number of residues.
[g] These proteins consist of two domains, and other ones are single domains.

Table S2: **Parameter values for $r_{\mathbf{cutoff}} \sim 8$ Å** employed for each protein family, and the averages of the total interactions ($\overline{\overline{\psi_N}}$) over all homologous sequences and of the means and the variances of interaction changes ($\overline{\overline{\Delta\psi_N}}$ and $\overline{\mathrm{Var}(\Delta\psi_N)}$) due to single nucleotide nonsynonymous mutations at all sites over all homologous sequences in each protein family.

Pfam family	L	p_c	n_c [a]	r_{cutoff} (Å)	$\bar{\psi}/L$ [b]	$\delta\psi^2/L$ [b]	$\overline{\overline{\psi_N}}/L$ [b]	$\overline{\overline{\Delta\psi_N}}$ [c]	$\overline{\mathrm{Var}(\Delta\psi_N)}$ [c]	r_{ψ_N} for $\overline{\overline{\Delta\psi_N}}$ [d]	α_{ψ_N}	r_{ψ_N} for $(\mathrm{Var}(\Delta\psi_N))^{1/2}$ [e]	α_{ψ_N}
HTH_3	53	0.175	7.434	8.22	−0.2039	2.8837	−3.0712	4.0412	30.8500	−0.94	−1.3671	−0.23	−0.1741
Nitroreductase	73	0.24	6.411	8.39	−0.1153	2.0825	−2.1975	2.9168	11.0879	−0.94	−1.3915	−0.59	−0.5270
SBP_bac_3	218	0.25	9.230	8.10	−0.1000	2.1624	−2.2618	3.1534	12.2140	−0.98	−1.5267	−0.84	−0.8111
SBP_bac_3	94	0.37	8.000	7.90	−0.1634	1.2495	−1.4054	1.8075	5.6101	−0.96	−1.4191	−0.65	−0.5171
OmpA	95	0.169	8.000	8.20	−0.2457	3.9093	−4.1542	6.0657	55.3105	−0.96	−1.5882	−0.47	−0.4471
DnaB	98	0.235	9.653	8.17	−0.2284	3.9976	−4.2291	6.1006	38.5736	−0.96	−1.4654	−0.52	−0.4385
LysR_substrate	191	0.23	7.843	7.87	−0.2248	1.4450	−1.6712	1.9999	6.7385	−0.97	−1.3646	−0.52	−0.5814
LysR_substrate	103	0.265	8.835	8.25	−0.2240	1.4132	−1.6372	2.0309	7.4763	−0.99	−1.4629	−0.78	−0.6311
Methyltransf_5	285	0.13	7.993	7.78	−0.1462	7.2435	−7.3887	12.2738	127.1400	−0.99	−1.7945	−0.08	−0.0461
Methyltransf_5	80	0.18	6.775	7.85	−0.1763	5.5162	−5.6896	8.7386	61.5293	−0.96	−1.5601	0.06	0.0612
SH3_1	48	0.14	6.417	8.01	−0.1348	3.9109	−4.0434	5.4273	39.8445	−0.94	−1.4457	−0.22	−0.1995
ACBP	80	0.22	9.175	8.24	−0.0525	4.6411	−4.7084	7.8272	55.1762	−0.97	−1.6189	−0.30	−0.1986
PDZ	81	0.205	9.061	8.16	−0.2398	3.1140	−3.3572	4.3897	21.0789	−0.96	−1.5014	−0.43	−0.3293
Copper-bind	125	0.23	9.232	8.26	−0.0838	4.1946	−4.2657	7.2514	51.7793	−0.98	−1.9254	−0.20	−0.1475

[a] The average number of contact residues per site within the cutoff distance; the center of side chain is used to represent a residue.
[b] M unique sequences without deletions are used with a sample weight (w_{σ_N}) for each sequence; w_{σ_N} is equal to the inverse of the number of sequences that are less than 20% different from a given sequence. The M and the effective number M_{eff} of the sequences are listed for each protein family in Table S1.
[c] Representatives of unique sequences without deletions, which are at least 20% different from each other, are used; the number of the representatives used is almost equal to M_{eff}. For HTH_3, 4431 sequences are used; abnormal sequences are removed.
[d] The correlation and regression coefficients of $\overline{\overline{\Delta\psi_N}}$ on ψ_N/L;see Eq. S93.
[e] The correlation and regression coefficients of $(\mathrm{Var}(\Delta\psi_N))^{1/2}$ on ψ_N/L.

Table S3: **Thermodynamic quantities estimated with $r_{\mathbf{cutoff}} \sim 8$ Å .**

Pfam family	r [a]	$k_B\hat{T}_s$ [a] (kcal/mol)	$\hat{T}_s$ (°K)	experimental T_m (°K)	$\hat{T}_g$ (°K)	T [b] (°K)	$\hat{\omega}$ [c] (k_B)	$\langle\Delta G_{ND}\rangle$ [d] (kcal/mol)
HTH_3	-	-	116.3	343.7	155.1	298	0.8107	−2.98
Nitroreductase	-	-	194.0	337.0	214.2	298	0.8537	−2.62
SBP_bac_3	-	-	184.8	336.1	207.0	298	0.8622	−8.14
SBP_bac_3	-	-	272.7	336.1	277.7	298	0.6025	−0.99
OmpA	-	-	86.9	320.0	126.8	298	0.9171	−3.16
DnaB	-	-	104.0	312.8	139.7	298	1.1082	−2.52
LysR_substrate	-	-	248.8	338.0	258.0	298	0.6722	−3.46
LysR_substrate	-	-	236.2	338.0	247.7	298	0.6425	−2.05
Methyltransf_5	-	-	57.3	375.0	107.8	298	1.0220	−39.91
Methyltransf_5	-	-	82.3	375.0	131.7	298	1.0783	−11.14
SH3_1	0.86	0.1583	102.3	344.0	143.8	295	0.9904	−3.68
ACBP	0.82	0.1169	87.0	324.4	127.6	278	1.0774	−6.51
PDZ	0.93	0.2794	140.7	312.9	168.5	298	1.0854	−1.81
Copper-bind	0.83	0.1781	89.8	359.3	135.8	298	0.9171	−11.55

[a] Reflective correlation (r) and regression ($k_B\hat{T}_s$) coefficients for least-squares regression lines of experimental $\Delta\Delta G_{ND}$ on $\Delta\psi_N$ through the origin.
[b] Temperatures are set up for comparison to be equal to the experimental temperatures for ΔG_{ND} or to 298°K if unavailable; see Table S4 for the experimental data.
[c] Conformational entropy per residue, in k_B units, in the denatured molten-globule state; see Eq. S20.
[d] Folding free energy in kcal/mol units; see Eq. S48.

Table S4: **Experimental data used.**

Pfam family	experimental values T_m (°K)	T (°K)	ΔG_{ND} (kcal/mol)	ref. for T_m	ref. for ΔG_{ND} and $\Delta\Delta G_{ND}$
HTH_3	343.7	298	-5.33 ± 0.36	(28)	(29)
Nitroreductase	337.0	-	-	(30)	
SBP_bac_3	336.1	-	-	(31)	
OmpA	320.0	-	-	(32)	
DnaB	312.8	-	-	(33)	
LysR_substrate	338.0	-	-	(34)	
Methyltransf_5	375.0	-	-	(35, 36)	
SH3_1	344.0	295	-3.70	(37)	(38)
ACBP	324.4	278	-8.08 ± 0.08	(39)	(40)
PDZ	312.9	298	-2.90	(41)	(26, 42)
Copper-bind	359.3	298	-12.90 ± 0.36	(27)	(43)

Table S5: **Parameter values for $r_{\mathbf{cutoff}} \sim 15.5$ Å** employed for each protein family, and the averages of the total interactions ($\overline{\overline{\psi_N}}$) over all homologous sequences and of the means and the variances of interaction changes ($\overline{\overline{\Delta\psi_N}}$ and $\overline{\mathrm{Var}(\Delta\psi_N)}$) due to single nucleotide nonsynonymous mutations at all sites over all homologous sequences in each protein family.

Pfam family	L	p_c	n_c [a]	r_{cutoff} (Å)	$\bar{\psi}/L$ [b]	$\delta\psi^2/L$ [b]	$\overline{\psi_N}/L$ [b]	$\overline{\overline{\Delta\psi_N}}$ [c]	$\overline{\mathrm{Var}(\Delta\psi_N)}$ [c]	r_{ψ_N} for $\overline{\overline{\Delta\psi_N}}$ [d]	α_{ψ_N}	r_{ψ_N} for $(\mathrm{Var}(\Delta\psi_N))^{1/2}$ [e]	α_{ψ_N}
HTH_3	53	0.24	32.30	15.46	−0.2591	4.0640	−4.3232	6.3128	48.5075	−0.93	−1.4723	−0.44	−0.2813
Nitroreductase	73	0.32	25.51	15.62	−0.1452	3.3359	−3.4815	5.2466	23.9884	−0.94	−1.5730	−0.68	−0.5961
SBP_bac_3	218	0.35	55.48	15.90	−0.0669	3.4004	−3.4674	5.5888	24.5240	−0.97	−1.6605	−0.84	−0.9034
SBP_bac_3	94	0.455	42.81	15.45	−0.1628	2.3208	−2.4831	3.8780	14.6360	−0.97	−1.6840	−0.77	−0.6742
OmpA	95	0.235	35.58	15.69	−0.2552	5.8175	−6.0757	9.5326	125.0540	−0.95	−1.6945	−0.44	−0.4231
DnaB	98	0.35	46.65	15.57	−0.2351	6.1890	−6.4167	10.3965	67.5994	−0.90	−1.5787	−0.33	−0.3279
LysR_substrate	191	0.33	44.16	15.13	−0.2668	2.3641	−2.6309	3.7028	14.7899	−0.96	−1.5508	−0.53	−0.4839
LysR_substrate	103	0.37	44.06	15.60	−0.2834	2.4271	−2.7111	3.8248	17.9478	−0.99	−1.5685	−0.84	−0.6683
Methyltransf_5	285	0.175	53.52	15.53	−0.1687	12.8982	−13.0658	23.2012	369.5520	−0.98	−1.7992	−0.14	−0.1249
Methyltransf_5	80	0.24	37.02	15.11	−0.1632	9.9944	−10.1576	16.9985	194.4250	−0.91	−1.6482	−0.38	−0.3845
SH3_1	48	0.165	28.46	15.76	−0.1350	7.6161	−7.7523	11.5955	187.9570	−0.92	−1.6770	−0.29	−0.2693
ACBP	80	0.28	36.27	15.34	−0.0235	7.4707	−7.4947	13.1960	102.0870	−0.92	−1.6896	0.12	0.1203
PDZ	81	0.33	40.82	15.77	−0.3022	5.2295	−5.5313	8.0540	62.2153	−0.97	−1.7009	−0.35	−0.2408
Copper-bind	125	0.295	44.34	15.43	−0.0934	8.5012	−8.5928	15.4936	102.3600	−0.97	−1.7939	−0.24	−0.2361

[a] The average number of contact residues per site within the cutoff distance; the center of side chain is used to represent a residue.
[b] M unique sequences without deletions are used with a sample weight (w_{σ_N}) for each sequence; w_{σ_N} is equal to the inverse of the number of sequences that are less than 20% different from a given sequence. The M and the effective number M_{eff} of the sequences are listed for each protein family in Table S1.
[c] Representatives of unique sequences without deletions, which are at least 20% different from each other, are used; the number of the representatives used is almost equal to M_{eff}. For HTH_3, 4461 sequences are used; abnormal sequences are removed.
[d] The correlation and regression coefficients of $\overline{\Delta\psi_N}$ on ψ_N/L;see Eq. S93.
[e] The correlation and regression coefficients of $(\mathrm{Var}(\Delta\psi_N))^{1/2}$ on ψ_N/L.

Table S6: **Thermodynamic quantities estimated with $r_{\mathbf{cutoff}} \sim 15.5$ Å .**

Pfam family	r [a]	$k_B\hat{T}_s$ [a] (kcal/mol)	$\hat{T}_s$ (°K)	experimental T_m (°K)	$\hat{T}_g$ (°K)	T [b] (°K)	$\hat{\omega}$ [c] (k_B)	$\langle\Delta G_{ND}\rangle$ [d] (kcal/mol)
HTH_3	-	-	92.3	343.7	135.4	298	0.9452	−3.73
Nitroreductase	-	-	131.3	337.0	165.8	298	1.0466	−4.30
SBP_bac_3	-	-	129.9	336.1	164.5	298	1.0601	−12.76
SBP_bac_3	-	-	168.1	336.1	194.1	298	0.8705	−3.86
OmpA	-	-	57.5	320.0	100.5	298	0.9516	−3.53
DnaB	-	-	78.2	312.8	118.2	298	1.3542	−3.32
LysR_substrate	-	-	167.2	338.0	193.8	298	0.8803	−8.38
LysR_substrate	-	-	151.8	338.0	181.9	298	0.8453	−4.64
Methyltransf_5	-	-	33.5	375.0	81.0	298	1.0994	−45.10
Methyltransf_5	-	-	46.1	375.0	96.0	298	1.1537	−12.95
SH3_1	0.84	0.0821	46.9	344.0	93.1	295	0.9678	−4.13
ACBP	0.82	0.0689	63.7	324.4	107.0	278	1.3220	−8.51
PDZ	0.94	0.1619	81.5	312.9	121.1	298	1.1852	−2.39
Copper-bind	0.89	0.0997	63.6	359.3	111.9	298	1.3710	−18.42

[a] Reflective correlation (r) and regression ($k_B\hat{T}_s$) coefficients for least-squares regression lines of experimental $\Delta\Delta G_{ND}$ on $\Delta\psi_N$ through the origin.

[b] Temperatures are set up for comparison to be equal to the experimental temperatures for ΔG_{ND} or to 298°K if unavailable; see Table S4 for the experimental data.

[c] Conformational entropy per residue, in k_B units, in the denatured molten-globule state; see Eq. S20.

[d] Folding free energy in kcal/mol units; see Eq. S48.

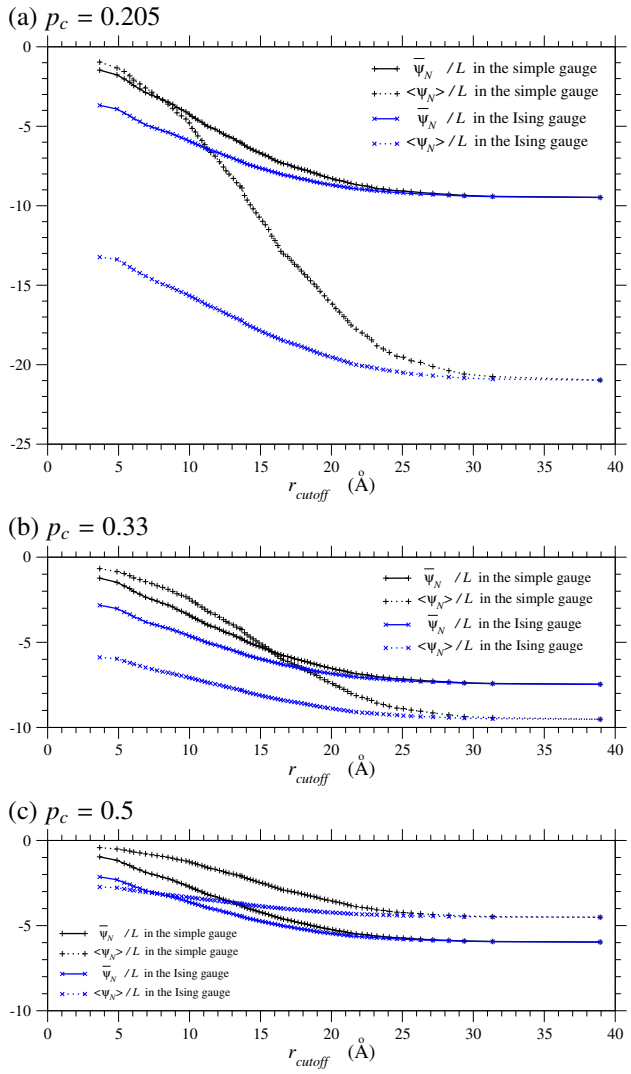
(a) p_c = 0.205
$\overline{\psi}_N$ /L in the simple gauge
<ψ_N>/L in the simple gauge
$\overline{\psi}_N$ /L in the Ising gauge
<ψ_N>/L in the Ising gauge
r_{cutoff} (Å)
(b) p_c = 0.33
$\overline{\psi}_N$ /L in the simple gauge
<ψ_N>/L in the simple gauge
$\overline{\psi}_N$ /L in the Ising gauge
<ψ_N>/L in the Ising gauge
r_{cutoff} (Å)
(c) p_c = 0.5
$\overline{\psi}_N$ /L in the simple gauge
<ψ_N>/L in the simple gauge
$\overline{\psi}_N$ /L in the Ising gauge
<ψ_N>/L in the Ising gauge
r_{cutoff} (Å)

Figure S1: **Dependences of the sample ($\overline{\psi_N}/L$) and ensemble ($\langle\psi_N\rangle_{\boldsymbol{\sigma}}/L$) averages of the total interaction per residue on the cutoff distance for pairwise interactions in the PDZ domain.** The ratios of pseudocount p_c = 0.205 and 0.33 are employed here for the cutoff distance $r_{\mathrm{cutoff}} \sim 8$ and 15.5Å respectively. The solid and dotted lines indicate the sample and ensemble averages, respectively, and black plus and blue cross marks show those for the simple and Ising gauges, respectively.

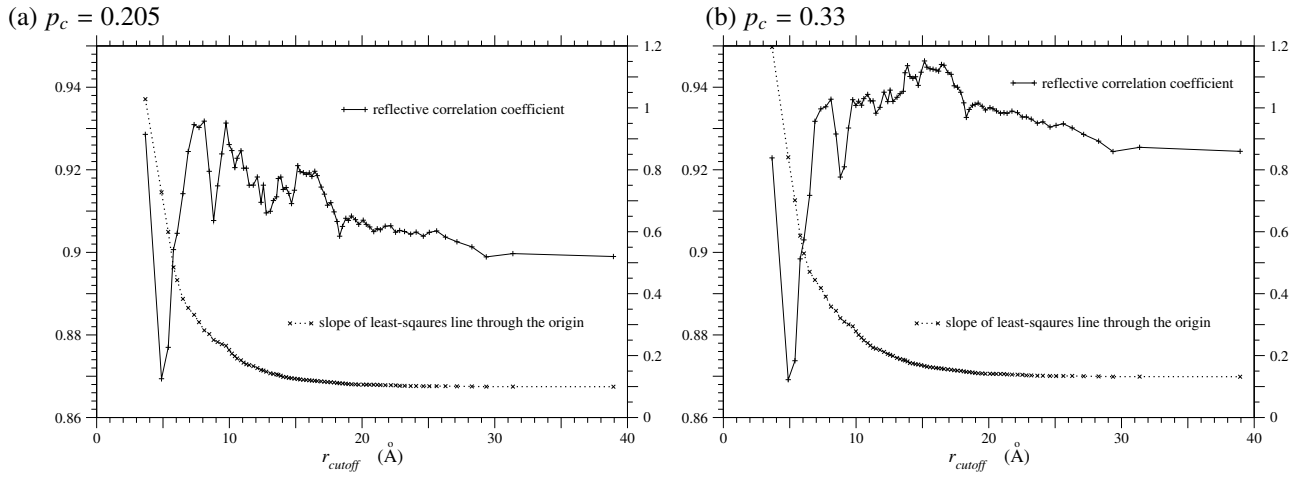

Figure S2: **Dependences of the reflective correlation and regression coefficients between the experimental $\Delta\Delta G_{ND}$ (26) and $\Delta\psi_N$ due to single amino acid substitutions on the cutoff distance for pairwise interactions in the PDZ domain.** The left and right figures are for the ratios of pseudocount, p_c = 0.205 and 0.33, respectively. The solid and dotted lines show the reflective correlation and regression coefficients for the least-squares regression line through the origin, respectively. The sample ($\overline{\psi_N}/L$) and ensemble ($\langle\psi_N\rangle_{\boldsymbol{\sigma}}/L$) averages of the total interaction agree with each other at the cutoff distance $r_{\mathrm{cutoff}} \sim 8$ Å for p_c = 0.205 and $r_{\mathrm{cutoff}} \sim 15.5$ Å for p_c = 0.33, where the reflective correlation coefficients attain to the maximum.

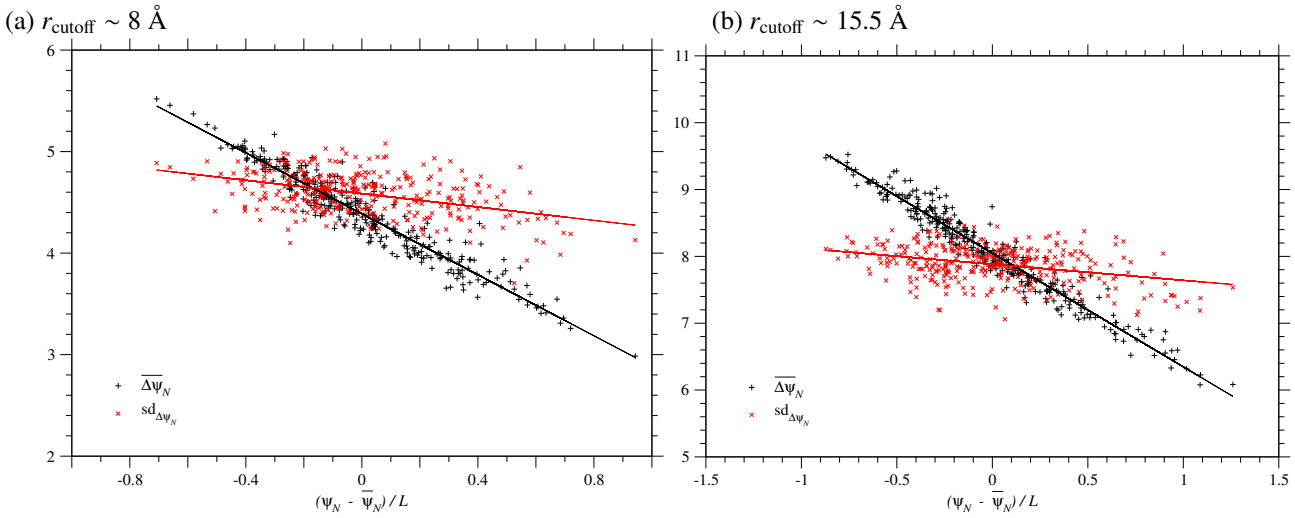

Figure S3: **Correlation between $\Delta\psi_N$ due to single nucleotide nonsynonymous substitutions and ψ_N of homologous sequences in the PDZ domain family.** The left and right figures correspond to the cutoff distance r_{cutoff} ~ 8 and 15.5Å respectively. Each of the black plus or red cross marks corresponds to the mean or the standard deviation of $\Delta\psi_N$ due to all types of single nucleotide nonsynonymous substitutions over all sites in each of the homologous sequences of the PDZ domain family. Only 335 representatives of unique sequences with no deletion, which are at least 20% different from each other, are employed; the number of the representatives is almost equal to M_{eff} in Table S1. The solid lines show the regression lines for the mean and the standard deviation of $\Delta\psi_N$.

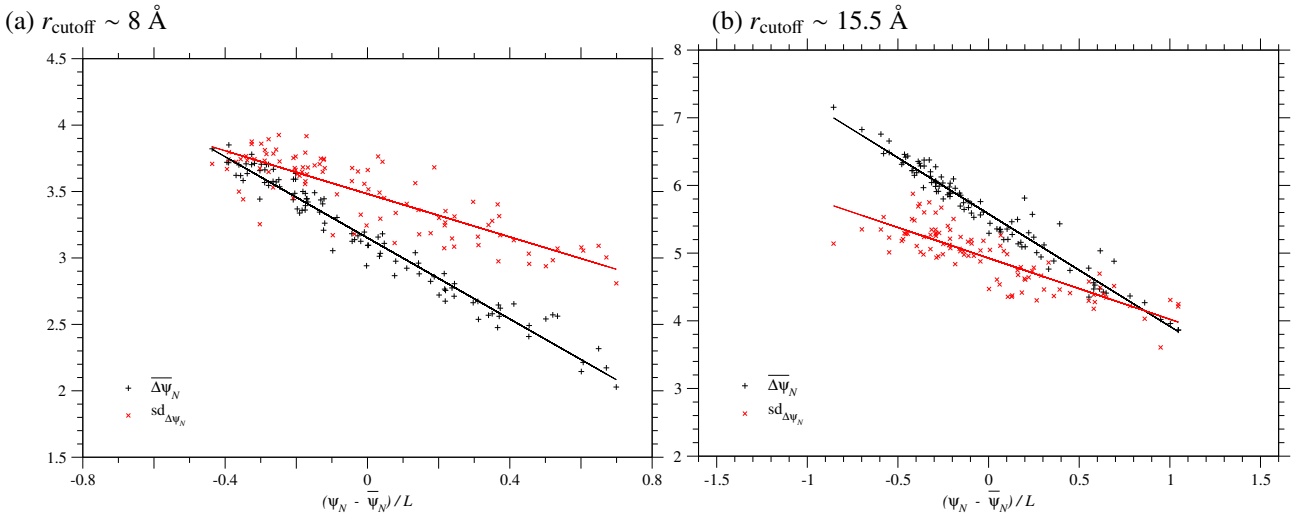

Figure S4: **Correlation between $\Delta\psi_N$ due to single nucleotide nonsynonymous substitutions and ψ_N of homologous sequences in the SBP_bac_3 family of the domain, 1WDN-A:5-222.** The left and right figures correspond to the cutoff distance r_{cutoff} ~ 8 and 15.5Å respectively. Each of the black plus or red cross marks corresponds to the mean or the standard deviation of $\Delta\psi_N$ due to all types of single nucleotide nonsynonymous substitutions over all sites in each of the homologous sequences in the SBP_bac_3 family of the domain, 1WDN-A:5-222. Only 100 representatives of unique sequences with no deletion, which are at least 20% different from each other, are employed; the number of the representatives is almost equal to M_{eff} in Table S1. The solid lines show the regression lines for the mean and the standard deviation of $\Delta\psi_N$.

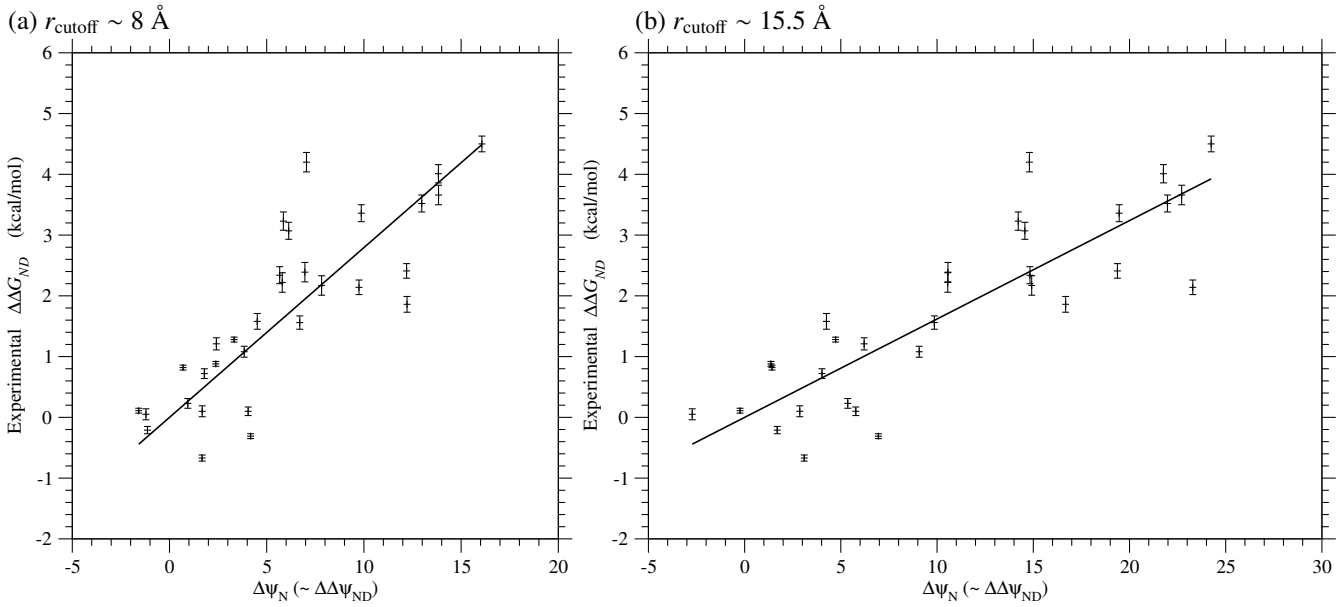

Figure S5: **Regression of the experimental values (26) of folding free energy changes ($\Delta\Delta G_{ND}$) due to single amino acid substitutions on $\Delta\psi_N(\simeq \Delta\Delta\psi_{ND})$ for the same types of substitutions in the PDZ domain.** The left and right figures correspond to the cutoff distance r_{cutoff} ~ 8 and 15.5Å respectively. The solid lines show the least-squares regression lines through the origin with the slopes, 0.279 kcal/mol for r_{cutoff} ~ 8Å and 0.162 kcal/mol for r_{cutoff} ~ 15.5 Å , which are the estimates of k_BT_s. The reflective correlation coefficients for them are equal to 0.93 and 0.94, respectively. The free energies are in kcal/mol units.

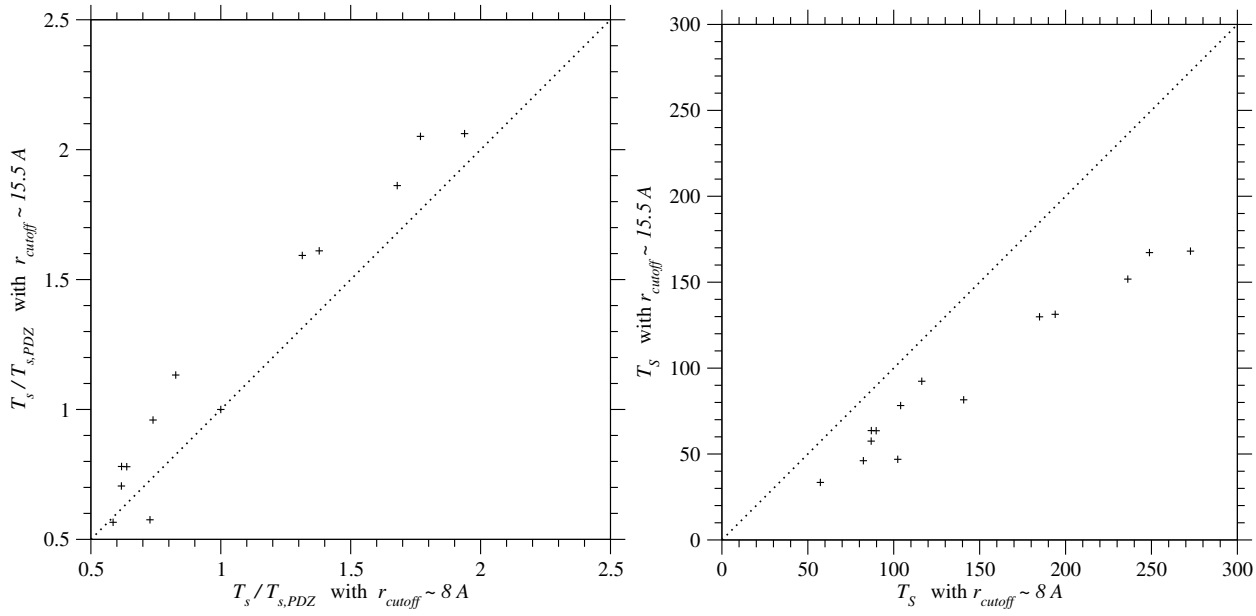

Figure S6: **Comparison of selection temperatures (T_s) estimated with different cutoff distances by the present method.** The abscissa and ordinate correspond to the cases of $r_{\text{cutoff}} \sim 8$ and 15.5Å respectively. The T_s is in °K units.

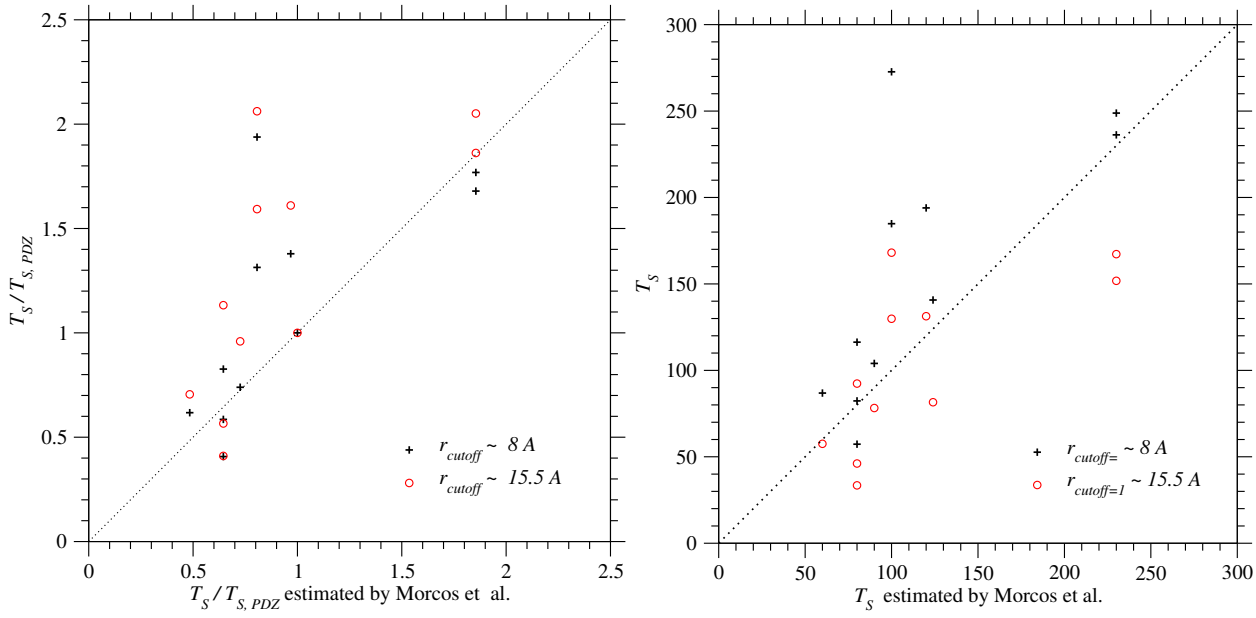

Figure S7: **Selection temperatures (T_s) estimated by the present method are plotted against those estimated by Morcos et al. (20). Plus and open circle marks correspond to the cases of $r_{\mathbf{cutoff}}$ ~ 8 and 15.5Å, respectively.**

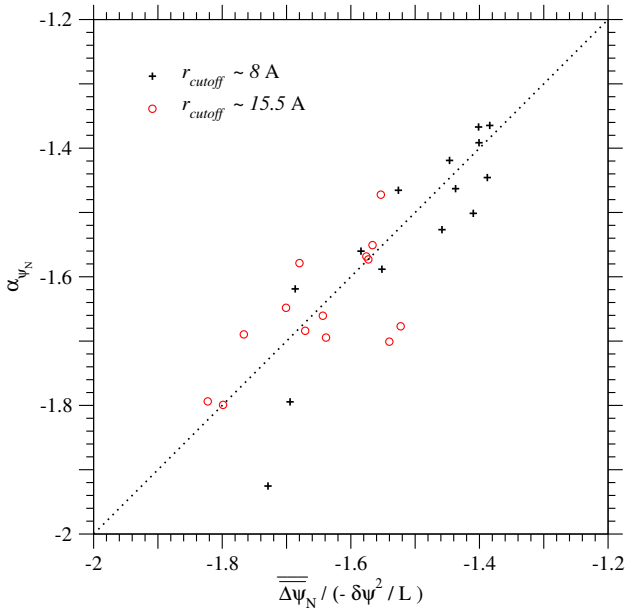

Figure S8: **Comparison of α_{ψ_N}, which is the regression coefficient of $\overline{\Delta\psi_N}$ on ψ_N/L, with $\overline{\overline{\Delta\psi_N}}/(-\delta\psi^2/L)$ for each protein family.** Plus and open circle marks correspond to the cases of $r_{\mathrm{cutoff}} \sim 8$ and 15.5Å, respectively.

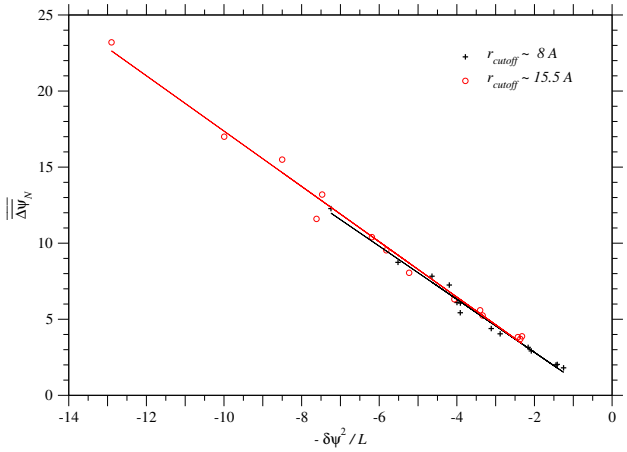

Figure S9: **Dependence of the average of $\overline{\Delta\psi_N}$ due to single nucleotide nonsynonymous substitutions over homologous sequences on $-\delta\psi^2/L$ across protein families.** Plus and open circle marks indicate the values for each protein family in the cases of $r_{\text{cutoff}} \sim 8$ and 15.5Å, respectively. In the case of the cutoff distance 8 Å, the correlation coefficient is equal to 0.99, and the regression line is $\overline{\overline{\Delta\psi_N(\sigma^N_{j\neq i}, \sigma^N_i \to \sigma_i)}} = -1.75(-\delta\psi^2/L) - 0.67$. In the case of $r_{\text{cutoff}} \sim 16$Å, the correlation coefficient is equal to 0.995, and the regression line is $\overline{\overline{\Delta\psi_N(\sigma^N_{j\neq i}, \sigma^N_i \to \sigma_i)}} = -1.82(-\delta\psi^2/L) - 0.81$.

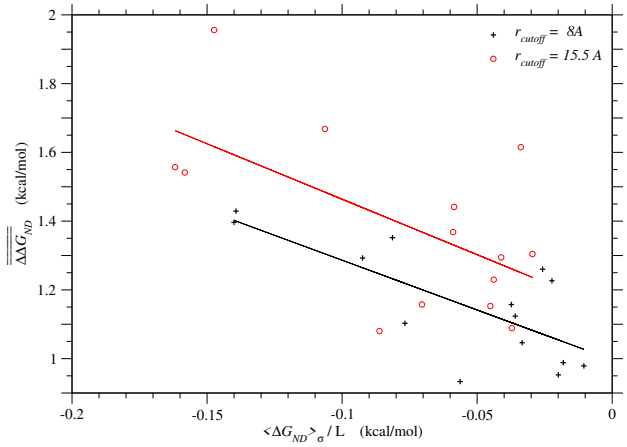

Figure S10: **The sample average of folding free energy change, $\overline{\overline{\Delta\Delta G_{ND}}} = k_B T_s \overline{\overline{\Delta\Delta\psi_{ND}}}$, is plotted against the ensemble average of folding free energy per residue, $\langle\Delta G_{ND}\rangle_\sigma/L = k_B T_s \langle\Delta\psi_{ND}\rangle_\sigma/L$, for each protein family.** In the case of the cutoff distance 8 Å, the correlation coefficient is $r = -0.74$, and the regression line is $\overline{\Delta\Delta G_{ND}(\sigma^N_{j\neq i}, \sigma^N_i \rightarrow \sigma_i)} = -2.90\langle\Delta G_{ND}\rangle_{\boldsymbol{\sigma}}/L + 1.00$. In the case of $r_{\text{cutoff}} \sim 16$ Å, the correlation coefficient is $r = -0.60$, and the regression line is $\overline{\Delta\Delta G_{ND}(\sigma^N_{j\neq i}, \sigma^N_i \rightarrow \sigma_i)} = -3.23\langle\Delta G_{ND}\rangle_{\boldsymbol{\sigma}}/L + 1.14$. The free energies are in kcal/mol units.

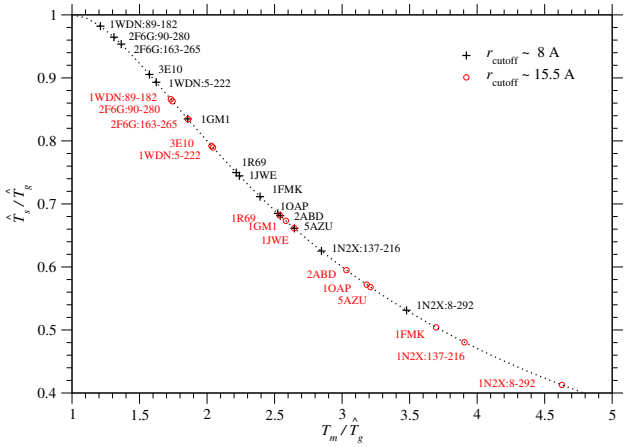

Figure S11: $\hat{T}_s/\hat{T}_g$ **is plotted against** $T_m/\hat{T}_g$ **for each protein domain.** A dotted curve corresponds to Eq. S51, $\hat{T}_s/\hat{T}_g = 2(T_m/\hat{T}_g)/((T_m/\hat{T}_g)^2 + 1)$. Plus and open circle marks indicate the values estimated with $r_{\text{cutoff}} \sim 8$ and 15.5Å , respectively. The T_s and T_g must satisfy $T_s < T_g < T_m$ for proteins to be able to fold into unique native structures.

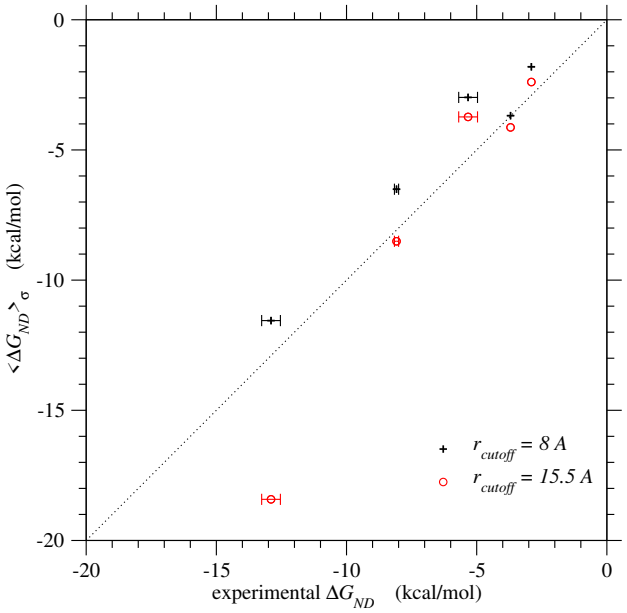

Figure S12: **Folding free energies, $\langle \Delta G_{ND} \rangle_{\sigma}$, predicted by the present method are plotted against their experimental values, $\Delta G_{ND}(\sigma_N)$.** The free energies are in kcal/mol units.

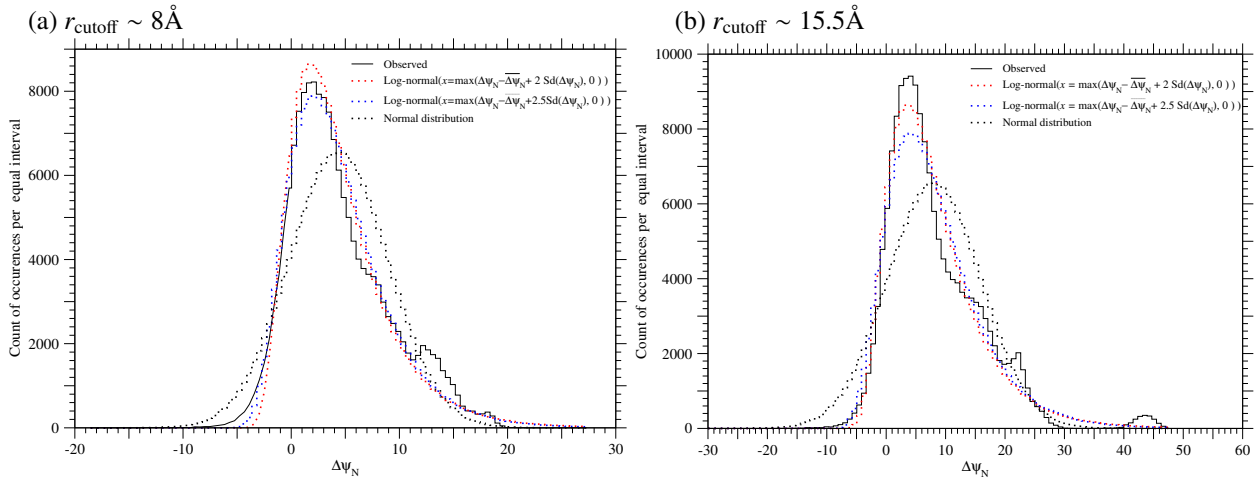

Figure S13: **The observed frequency distribution and the fitted distributions of $\Delta\psi_N$ in the PDZ protein family.** A black solid line indicates the observed frequency distribution of $\Delta\psi_N$ per equal interval in homologous sequences of the PDZ protein family, and red dotted and blue dotted lines indicate the total frequencies of log-normal distributions with $n_{\mathrm{shift}} = 2$ or 2.5 and parameters estimated with the mean and variance of the observed distribution for each protein; see Eqs. S78 and S82. A black dotted line indicates the total frequencies of normal distributions the mean and variance of which are equal to those of the observed distribution for each protein. Only representatives of unique sequences with no deletion, which are at least 20% different from each other, are employed; the total count is equal to 164651 over 335 homologous sequences, which is almost equal to M_{eff} in Table S1.

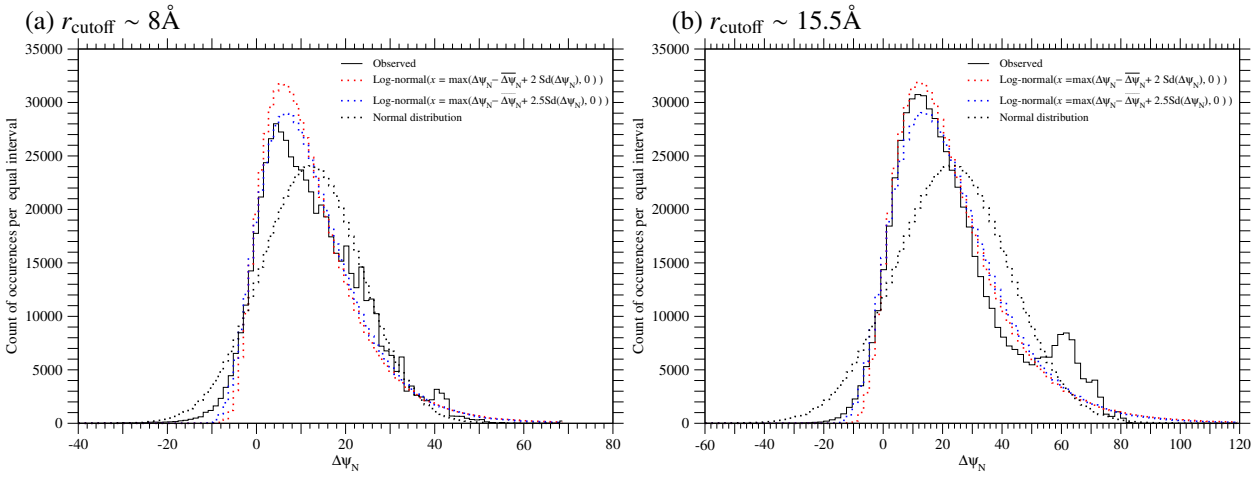
(a) r_{cutoff} ~ 8Å
(b) r_{cutoff} ~ 15.5Å
Count of occurences per equal interval
$\Delta\psi_N$
Observed
Log-normal(x = max(Δψ_N − Δψ̄_N + 2 Sd(Δψ_N), 0))
Log-normal(x = max(Δψ_N − Δψ̄_N + 2.5Sd(Δψ_N), 0))
Normal distribution

Figure S14: **The observed frequency distribution and the fitted distribution of $\Delta\psi_N$ in the Methyltransf_5 family of the domain, 1N2X-A:8-292.** A black solid line indicates the observed frequency distribution of $\Delta\psi_N$ per equal interval in homologous sequences of the Methyltransf_5 protein family, and red dotted and blue dotted lines indicate the total frequencies of log-normal distributions with $n_{\mathrm{shift}} = 2$ or 2.5 and parameters estimated with the mean and variance of the observed distribution for each protein; see Eqs. S78 and S82. A black dotted line indicates the total frequencies of normal distributions the mean and variance of which are equal to those of the observed distribution for each protein. Only representatives of unique sequences with no deletion, which are at least 20% different from each other, are employed; the total count is equal to 604510 over 354 homologous sequences, which is almost equal to M_{eff} in Table S1.

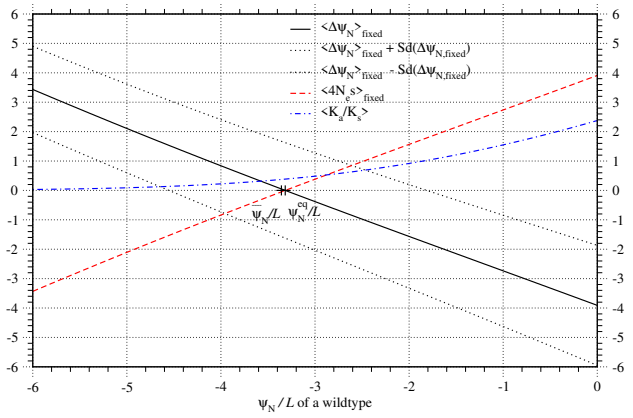

Figure S15: **The average of $\Delta\psi_N(\simeq \Delta\Delta\psi_{ND})$ over fixed single nucleotide nonsynonymous mutations versus ψ_N/L of a wildtype for the PDZ protein family.** The averages of $\Delta\psi_N(\simeq \Delta\Delta\psi_{ND})$ and $4N_e s$ over the fixed mutants, and the average of $K_a/K_s(\equiv u(s)/u(0))$ over all the mutants are plotted against ψ_N/L of a wildtype by solid, broken, and dash-dot lines, respectively; $q_m = 1/(2\times 10^6)$ is assumed. Dotted lines show the values of $\langle\Delta\psi_N\rangle_{\rm fixed} \pm$ sd, where the sd is the standard deviation of $\Delta\psi_N$ over fixed mutants. Fixation probability has been calculated in the approximation of $\Delta\Delta\psi_{ND} \simeq \Delta\psi_N$; see Eqs. S23 and S38. Here the empirical relationships of Eqs. S93 and S95 are assumed; that is, the mean of $\Delta\psi_N$ linearly decreases as ψ_N increases, but the variance of $\Delta\psi_N$ is constant irrespective of ψ_N. The slope (α_{ψ_N}) and intercept ($\overline{\overline{\Delta\psi_N}}$) and the average of the variance of $\Delta\psi_N$ over homologous sequences that are estimated with $r_{\rm cutoff} \sim 8$Å for the PDZ and listed in Table S2 are employed here. The distribution of $\Delta\psi_N$ due to single nucleotide nonsynonymous mutations is approximated by a log-normal distribution with $n_{\rm shift} = 2.0$; see Eqs. S78 and S82. The $\psi_N^{\rm eq}$, where $\langle\Delta\Delta\psi_{ND}\rangle_{\rm fixed} \simeq \langle\Delta\psi_N\rangle_{\rm fixed} = 0$, is the stable equilibrium value of ψ_N in the protein evolution of the PDZ protein family. The $\psi_N^{\rm eq}$ is close to the average of ψ_N over homologous sequences ($\overline{\psi_N}$), indicating that the present approximations for $\psi_N^{\rm eq}$ and for $\overline{\psi_N} = \langle\psi_N\rangle_{\boldsymbol{\sigma}}$ are consistent to each other.

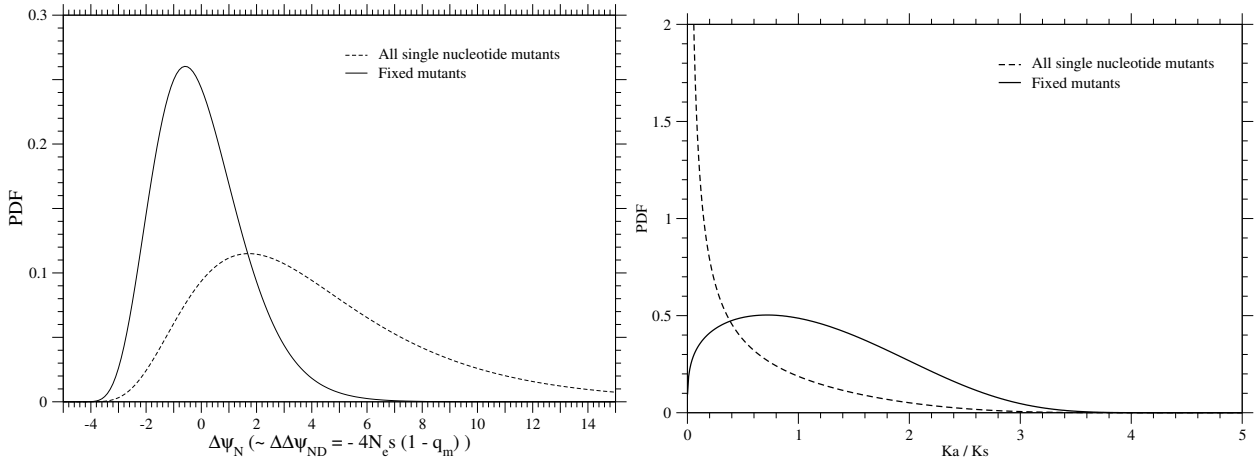

Figure S16: **PDFs of $\Delta\psi_N(\simeq \Delta\Delta\psi_{ND} = -4N_e s(1-q_m))$ and of K_a/K_s for all single nucleotide nonsynonymous mutants and for their fixed mutants at equilibrium ($\langle\Delta\psi_N\rangle_{\mathbf{fixed}} = 0$) for the PDZ protein family.** K_a/K_s is defined as the ratio of nonsynonymous to synonymous substitution rate per site, $u(s)/u(0)$; see Eq. S85. Fixation probability has been calculated in the approximation of $\Delta\Delta\psi_{ND} \simeq \Delta\psi_N$; see Eqs. S23 and S38. The equilibrium value $\psi_N^{\rm eq}$, where $\langle\Delta\Delta\psi_{ND}\rangle_{\rm fixed} \simeq \langle\Delta\psi_N\rangle_{\rm fixed} = 0$, is calculated by using the linear dependency of $\overline{\Delta\psi_N}$ on ψ_N (Eq. S93) and estimated values with $r_{\rm cutoff} \sim 8$Å for the PDZ in Tables S2. The variance of $\Delta\psi_N$ is approximated to be constant and equal to $\overline{\rm Var(\Delta\psi_N)}$; see Eq. S95. The distribution of $\Delta\psi_N$ due to single nucleotide nonsynonymous mutations is approximated by a log-normal distribution with $n_{\rm shift} = 2.0$; see Eqs. S78 and S82.

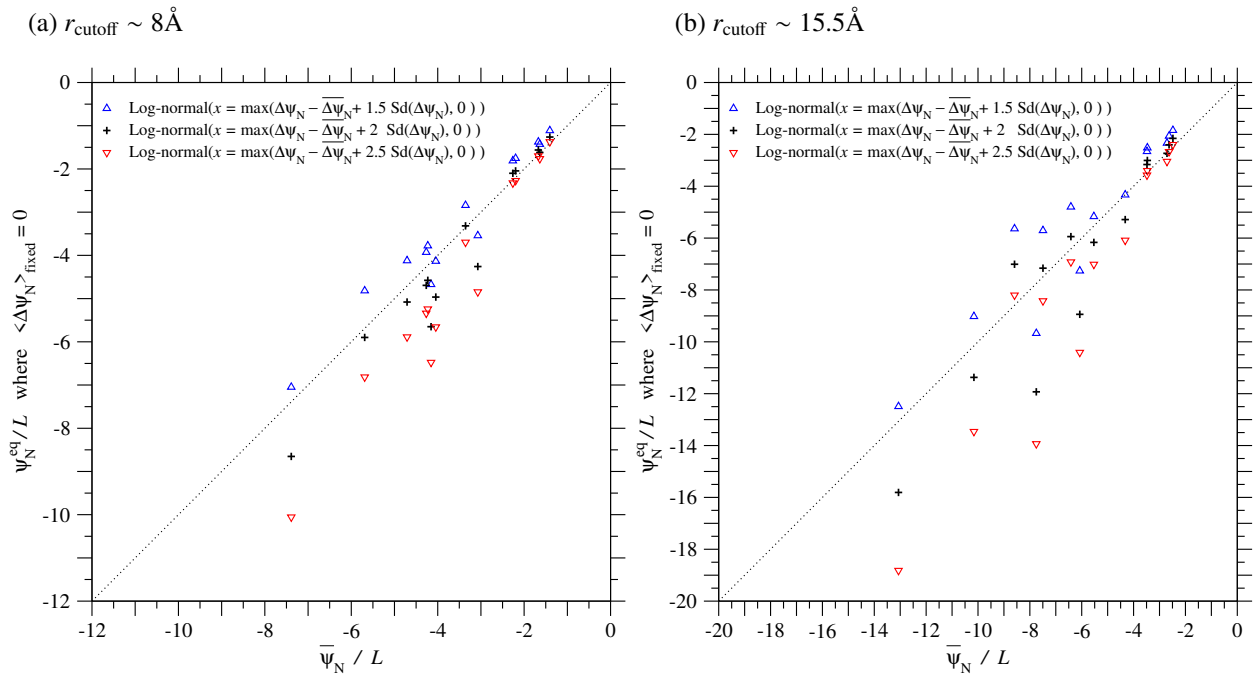
(a) $r_{\rm cutoff}$ ~ 8Å
(b) $r_{\rm cutoff}$ ~ 15.5Å
Log-normal(x = max($\Delta\psi_N - \overline{\Delta\psi_N}$+ 1.5 Sd($\Delta\psi_N$), 0))
Log-normal(x = max($\Delta\psi_N - \overline{\Delta\psi_N}$ + 2 Sd($\Delta\psi_N$), 0))
Log-normal(x = max($\Delta\psi_N - \overline{\Delta\psi_N}$+ 2.5 Sd($\Delta\psi_N$), 0))
$\psi_N^{\rm eq}/L$ where $\langle\Delta\psi_N\rangle_{\rm fixed} = 0$
$\overline{\psi}_N / L$

Figure S17: **The equilibrium value of ψ_N/L, where $\langle\Delta\psi_N\rangle_{\rm fixed} = 0$, is plotted against the average of ψ_N/L over homologous sequences for each protein family.** The cutoff distances, (a) $r_{\rm cutoff} = 8$Å and (b) $r_{\rm cutoff} = 15.5$Å are employed to estimate ψ_N of each protein family. The equilibrium values $\psi_N^{\rm eq}$, where $\langle\Delta\psi_N\rangle_{\rm fixed} = 0$, are calculated by using the linear dependency of $\overline{\Delta\psi_N}$ on ψ_N (Eq. S93) and estimated values with $r_{\rm cutoff} \sim 8$ or 15.5Å in Tables S2 or S5. The variance of $\Delta\psi_N$ is approximated to be constant and equal to $\overline{\rm Var(\Delta\psi_N)}$; see Eq. S95. Plus, upper triangle, and lower triangle marks indicate the cases of log-normal distributions with $n_{\rm shift} = 1.5$, 2.0, and 2.5 employed to approximate the distribution of $\Delta\psi_N$, respectively; see Eqs. S78 and S82.

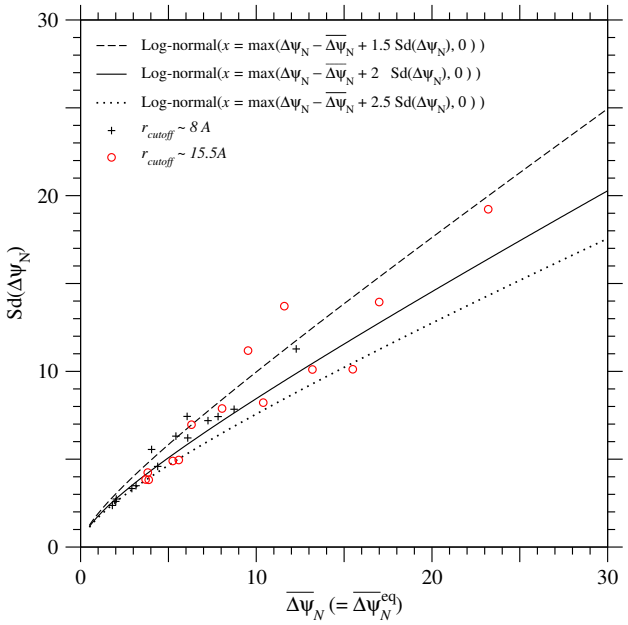
Log-normal(x = max(Δψ_N − Δψ_N + 1.5 Sd(Δψ_N), 0))
Log-normal(x = max(Δψ_N − Δψ_N + 2 Sd(Δψ_N), 0))
Log-normal(x = max(Δψ_N − Δψ_N + 2.5 Sd(Δψ_N), 0))
r_cutoff ~ 8 A
r_cutoff ~ 15.5A
Sd(Δψ_N)
Δψ_N (= Δψ_N^eq)
0
10
20
30

Figure S18: **Relationship between the mean and the standard deviation of $\Delta\psi_N$ due to single nucleotide nonsynonymous mutations at equilibrium,** $\langle\Delta\psi_N\rangle_{\mathbf{fixed}} = 0$ The standard deviation of $\Delta\psi_N$ that satisfies $\langle\Delta\psi_N\rangle_{\text{fixed}} = 0$ is plotted against its mean, $\overline{\Delta\psi_N}$. Broken, solid, and dotted lines indicate the cases of log-normal distributions with $n_{\text{shift}} = 1.5, 2.0$ and 2.5 employed to approximate the distribution of $\Delta\psi_N$, respectively; see Eqs. S78 to S82. Plus and open circle marks indicate the averages, $\overline{\overline{\Delta\psi_N}}$ and $\overline{\text{Var}(\Delta\psi_N)}^{1/2}$, over homologous sequences in each protein family for $r_{\text{cutoff}} \sim 8$ and 15.5Å, respectively; see Tables S2 and S5.

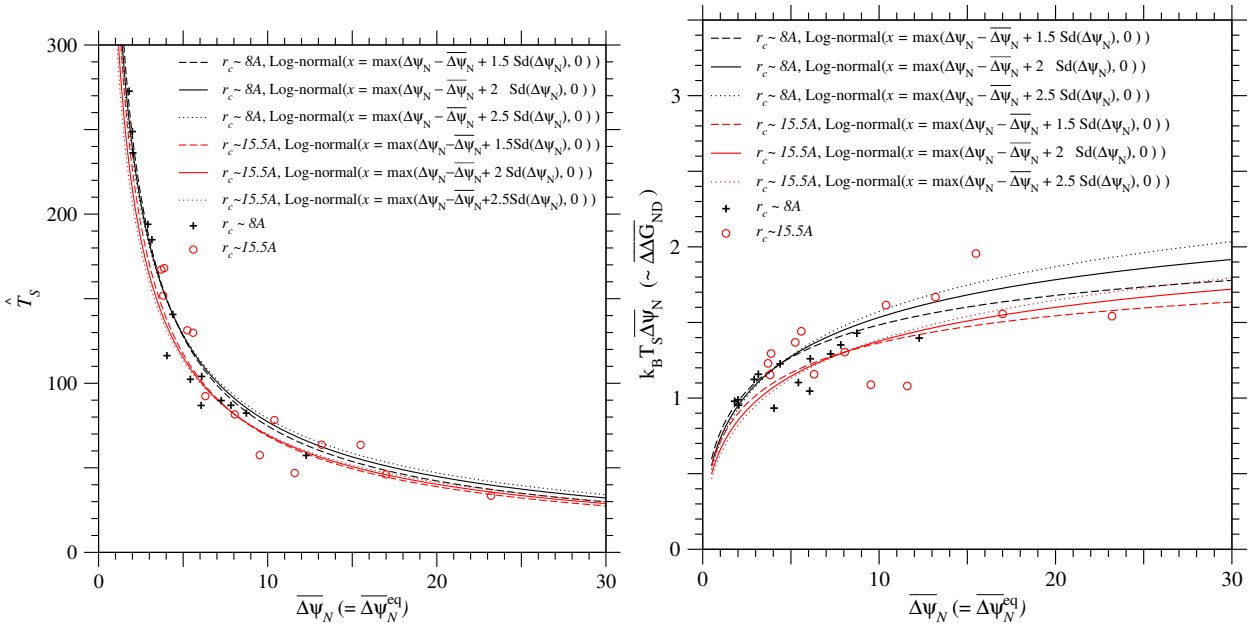
r_c~ 8A, Log-normal(x = max($\Delta\psi_N - \overline{\Delta\psi}_N$ + 1.5 Sd($\Delta\psi_N$), 0))
r_c~ 8A, Log-normal(x = max($\Delta\psi_N - \overline{\Delta\psi}_N$ + 2 Sd($\Delta\psi_N$), 0))
r_c~ 8A, Log-normal(x = max($\Delta\psi_N - \overline{\Delta\psi}_N$ + 2.5 Sd($\Delta\psi_N$), 0))
r_c~15.5A, Log-normal(x = max($\Delta\psi_N - \overline{\Delta\psi}_N$ + 1.5Sd($\Delta\psi_N$), 0))
r_c~15.5A, Log-normal(x = max($\Delta\psi_N - \overline{\Delta\psi}_N$ + 2 Sd($\Delta\psi_N$), 0))
r_c~15.5A, Log-normal(x = max($\Delta\psi_N - \overline{\Delta\psi}_N$ +2.5Sd($\Delta\psi_N$), 0))
r_c ~ 8A
r_c~15.5A
$\hat{T}_s$
$\overline{\Delta\psi}_N$ (= $\overline{\Delta\psi}_N^{eq}$)
$k_B T_s \overline{\Delta\psi}_N$ (~ $\overline{\Delta\Delta G}_{ND}$)

Figure S19: **Relationships between $\hat{T}_s$ and $\overline{\Delta\psi_N}$ and between $k_B T_s \overline{\Delta\psi_N}$($\simeq \overline{\Delta\Delta\hat{G}_{ND}}$) and $\overline{\Delta\psi_N}$ at equilibrium, $\langle\Delta\psi_N\rangle_{\mathbf{fixed}} = 0$.** The estimate $\hat{T}_s$ of effective temperature for selection and the estimate of mean folding free energy change, $k_B T_s \overline{\Delta\psi_N} \simeq \overline{\Delta\Delta\hat{G}_{ND}}$, are plotted against $\overline{\Delta\psi_N}$ under the condition of $\langle\Delta\psi_N\rangle_{\text{fixed}} = 0$. The T_s is estimated in relative to the T_s of the PDZ family in the approximation (11) that the variance of ΔG_N due to single nucleotide nonsynonymous mutations is constant irrespective of protein families; see Eq. S97. Broken, solid, and dotted lines indicate the cases of log-normal distributions with $n_{\text{shift}} = 1.5, 2.0$ and 2.5 employed to approximate the distribution of $\Delta\psi_N$, respectively; see Eqs. S78 to S82. Plus and open circle marks indicate those estimates against the average of $\overline{\Delta\psi_N}$ over homologous sequences for each protein family with $r_{\text{cutoff}} \sim 8$ and 15.5Å, respectively; see Tables S2 and S5.

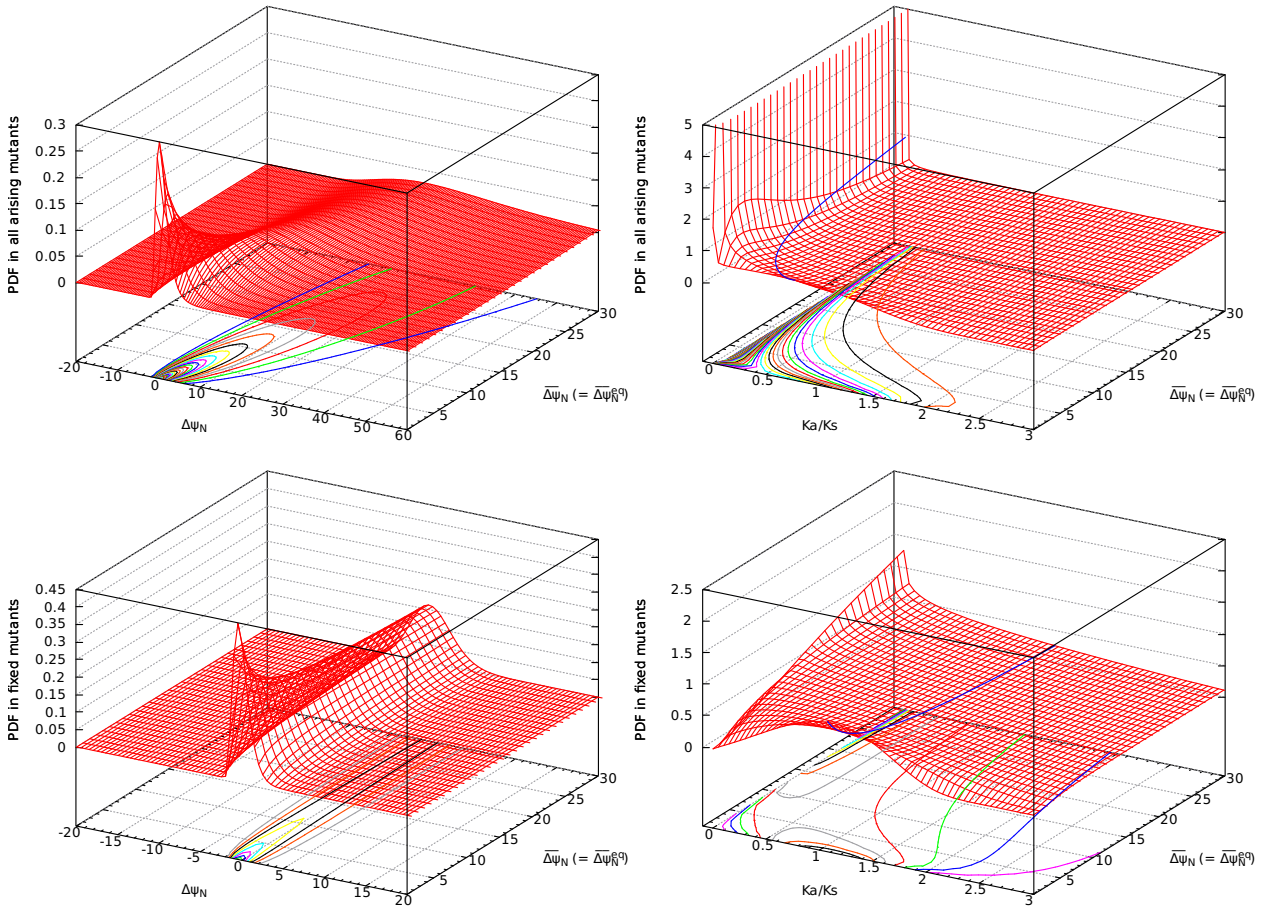

Figure S20: **PDFs of $\Delta\psi_N$ and K_a/K_s in all singe nucleotide nonsynonymous mutants and in their fixed mutants as a function of $\overline{\Delta\psi_N}$ at equilibrium, $\langle\Delta\psi_N\rangle_{\mathbf{fixed}} = 0$.** Fixation probability has been calculated in the approximation of $\Delta\Delta\psi_{ND} \simeq \Delta\psi_N$; see Eqs. S23 and S38. The distribution of $\Delta\psi_N$ due to single nucleotide nonsynonymous mutations is approximated by a log-normal distribution with $n_{\rm shift} = 2.0$; see Eqs. S78 and S82. The standard deviation of $\Delta\psi_N$ is determined to satisfy $\langle\Delta\psi_N\rangle_{\rm fixed} = 0$ at $\overline{\Delta\psi_N} = \overline{\Delta\psi_N}^{\rm eq}$.

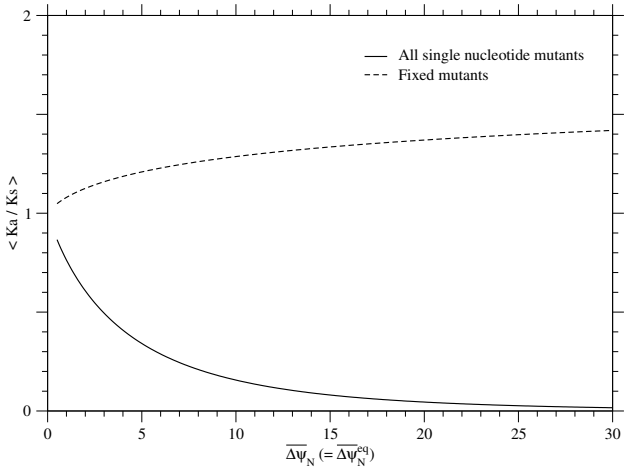

Figure S21: **The averages of K_a/Ks over all single nucleotide nonsynonymous mutations and over their fixed mutations as a function of $\overline{\Delta\psi_N}$ at equilibrium, $\langle\Delta\psi_N\rangle_{\mathbf{fixed}} = 0$.** Solid and broken lines indicate $\langle K_a/K_s\rangle$ and $\langle K_a/K_s\rangle_{\rm fixed}$, respectively. Fixation probability has been calculated in the approximation of $\Delta\Delta\psi_{ND} \simeq \Delta\psi_N$; see Eqs. S23 and S38. The distribution of $\Delta\psi_N$ due to single nucleotide nonsynonymous mutations is approximated by a log-normal distribution with $n_{\rm shift} = 2.0$; see Eqs. S78 and S82. The standard deviation of $\Delta\psi_N$ is determined to satisfy $\langle\Delta\psi_N\rangle_{\rm fixed} = 0$ at $\overline{\Delta\psi_N} = \overline{\Delta\psi_N}^{\rm eq}$.

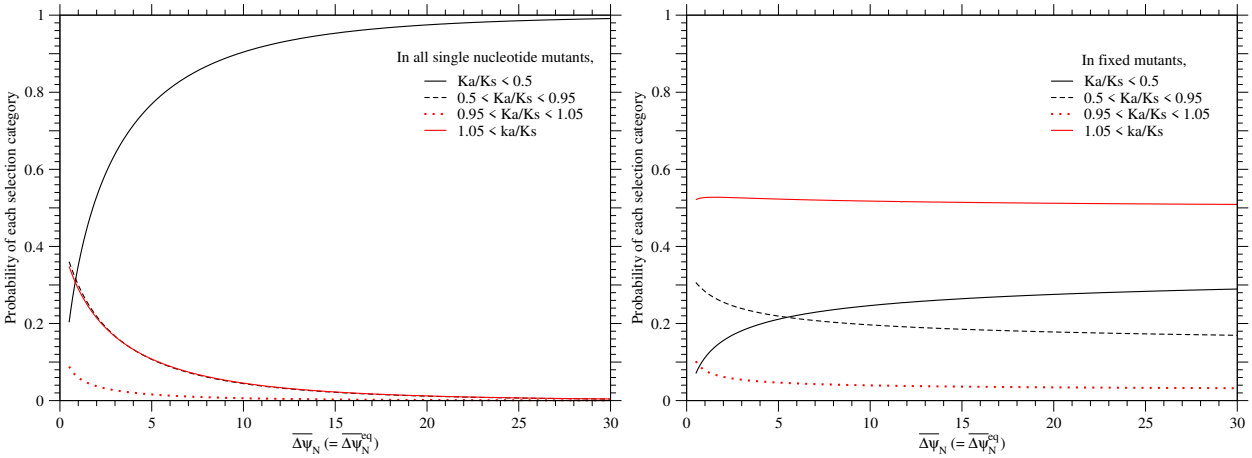
In all single nucleotide mutants,
Ka/Ks < 0.5
0.5 < Ka/Ks < 0.95
0.95 < Ka/Ks < 1.05
1.05 < ka/Ks
In fixed mutants,
Ka/Ks < 0.5
0.5 < Ka/Ks < 0.95
0.95 < Ka/Ks < 1.05
1.05 < ka/Ks
Probability of each selection category
$\overline{\Delta\psi_N}$ (= $\overline{\Delta\psi_N^{eq}}$)

Figure S22: **The probabilities of each selection category in all single nucleotide nonsynonymous mutations and in their fixed mutations as a function of $\overline{\Delta\psi_N}$ at equilibrium, $\langle\Delta\psi_N\rangle_{\mathbf{fixed}} = 0$.** The left and right figures are for single nucleotide nonsynonymous mutations and for their fixed mutations, respectively. Red solid, red dotted, black broken, and black solid lines indicate positive, neutral, slightly negative and negative selection categories, respectively; the values of K_a/K_s are divided arbitrarily into four categories, $K_a/K_s > 1.05$, $1.05 > K_a/K_s > 0.95$, $0.95 > K_a/K_s > 0.5$, and $0.5 > K_a/K_s$, which correspond to their selection categories, respectively. Fixation probability has been calculated in the approximation of $\Delta\Delta\psi_{ND} \simeq \Delta\psi_N$; see Eqs. S23 and S38. The distribution of $\Delta\psi_N$ due to single nucleotide nonsynonymous mutations is approximated by a log-normal distribution with $n_{\rm shift} = 2.0$; see Eqs. S78 and S82. The standard deviation of $\Delta\psi_N$ is determined to satisfy $\langle\Delta\psi_N\rangle_{\rm fixed} = 0$ at $\overline{\Delta\psi_N}(= \overline{\Delta\psi_N}^{\rm eq})$.

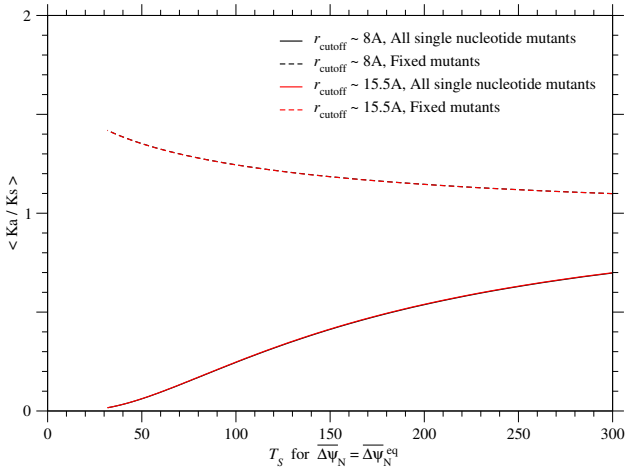

Figure S23: **The averages of K_a/Ks over all single nucleotide nonsynonymous mutations and over their fixed mutations as a function of the effective temperature of selection, T_s, at equilibrium, $\langle\Delta\psi_N\rangle_{\mathbf{fixed}} = 0$.** Solid and broken lines indicate $\langle K_a/K_s\rangle$ and $\langle K_a/K_s\rangle_{\rm fixed}$, respectively. Fixation probability has been calculated in the approximation of $\Delta\Delta\psi_{ND} \simeq \Delta\psi_N$; see Eqs. S23 and S38. The distribution of $\Delta\psi_N$ due to single nucleotide nonsynonymous mutations is approximated by a log-normal distribution with $n_{\rm shift} = 2.0$; see Eqs. S78 and S82. The standard deviation of $\Delta\psi_N$ is determined to satisfy $\langle\Delta\psi_N\rangle_{\rm fixed} = 0$ at $\overline{\Delta\psi_N}(= \overline{\Delta\psi_N}^{\rm eq})$. The T_s is estimated in the scale relative to the T_s of the PDZ family in the approximation (11) that the variance of ΔG_N due to single nucleotide nonsynonymous mutations is constant irrespective of protein families; see Eq. S97. The curves for $r_{\rm cutoff} \sim 8$ and 15.5Å almost overlap with each other.